BMC Plant Biology

RESEARCH

Open Access

Investigation of mechanisms underlying seedlessness in a Sangiovese somatic variant through comparative genomic and histological analyses

Paula Moreno-Sanz[1*†], Laura Costantini[2†], Silvia Lorenzi[2], Elvira D'Amato[3], Tomas Roman[4], Mara Miculan[5,6,9], Gabriele Magris[5,6], Gabriele Di Gaspero[6], Anna Nebish[7,8] and Maria Stella Grando[1]

Abstract

Background Both parthenocarpy and stenospermocarpy lead to seedless grapes. Only parthenocarpy, which is rather rare, generates berries with a complete absence of seed tissues. Stenospermocarpy, which is instead more common, produces berries with seed traces because seed development is promoted by embryo formation and then arrested by its abortion. In viticulture, parthenocarpic varieties account for a minority of the production of seedless table grapes, while they are more commonly used for raisins and very rarely for winemaking. Parthenocarpy is the putative cause of seedlessness in Corinto Nero, a bud sport of the seeded winegrape Sangiovese. In our previous studies, embryo sac abnormalities arising from meiotic disorders were accompanied by transcriptional changes in gene functions linked to gametophyte development and ovule fertilization. Here, with the aim of elucidating the cause of parthenocarpy in Corinto Nero, comparative histological and genomic analyses were performed.

Results Histologically, Corinto Nero showed abnormalities in megasporogenesis and the arrest of female gametophyte development very early during the megagametogenesis, compared to seeded Sangiovese. Genetically, Corinto Nero showed putative private mutations in candidate genes with functions related to cell cycle, meiosis and mitosis, compared to ten Sangiovese bud sports, which differed phenotypically from one another and from Corinto Nero for diverse traits, but they all were seeded. One of these mutations was validated in a *Disrupted Meiotic cDNA1* homolog gene, which has a missense variant and a significant lower expression at key reproductive developmental stages in Corinto Nero.

Conclusions This work provided a list of candidate genes with somatic mutations in Corinto Nero that possibly impair sporogenesis and gametogenesis, preventing seed development. Sangiovese has a genetic predisposition to develop ovary disorders, and to forcibly set fruit in absence of pollination, which may have been turned into full

†Paula Moreno-Sanz and Laura Costantini contributed equally to this work.

*Correspondence:
Paula Moreno-Sanz
paula.morenosanz@gmail.com

Full list of author information is available at the end of the article

expression of parthenocarpy in Corinto Nero by further mutations. A systematic genome editing of the candidate genes in the seeded Sangiovese will be required for their functional validation.

Keywords Parthenocarpy, Corinto Nero, Sangiovese, Megasporogenesis, Megagametogenesis, Disrupted meiotic progression, *DMC*1

Background

Somatic variation is an important source of phenotypic diversity in vegetatively propagated crops. This variation contributes to some differentiation within each cultivar, which may also provide favorable changes for adapting to challenging environmental conditions and meeting new market demands, especially in grapevine. This crop requires, indeed, lengthy breeding cycles and, on top of that, the wine industry is rigid against embracing new breeds. By having a nearly identical genetic background to the original seedling, somatic variants also serve as near-isogenic lines for research in genetics and physiology to understand the molecular basis of trait variation, which in turn enables precision breeding [1, 2].

In viticulture, the phenotypic variation arising from spontaneous somatic mutations that accumulate during vegetative propagation has been selected over time to differentiate clonal lineages within traditional varieties, which are referred to by grape connoisseurs, multiplied by nurseries, and planted by vine growers as "clones". Up to now, clonal selection has provided the only means to incorporate novel diversity into the cultivated germplasm, while maintaining the identity of each cultivar. Examples of relevant grapevine mutations that originated from somatic variation and were characterized down to the molecular level are those affecting berry color, Muscat flavor, seed and berry development [3–6].

Somatic mutations in grapevine range from single nucleotide polymorphisms (SNPs) and small insertions/deletions (InDels < 50 bp) to structural variations (SVs), including inter- and intra-chromosomal translocations, deletions, and insertions (> 1 kb), and even chromothripsis [7–9]. Variant phenotypes were frequently associated with the movement of transposable elements (TEs) altering the expression of the genes into or nearby which they jump or from which they excise [1, 10–14]. Given this breadth of mutational events, the identification and characterization of somatic variation requires genome-wide analyses [15]. Identifying *bona-fide* somatic variation between grapevine bud sports is challenging, because the frequency at which it occurs is orders of magnitude lower than sequence variation between any two grapevine cultivars. Comparing a mutant for the phenotype of interest with a group of other unrelated mutants of the same cultivar for other phenotypic traits, as opposed to using pairwise comparisons, is a means to increase the statistical power for filtering out false positives caused by sequencing errors, read misalignments, multiple mappings, and other inherent technical biases.

Two types of seedlessness are reported in grapevine: (i) stenospermocarpy, in which ovule fertilization takes place but the embryos abort and/or the endosperm or the seed coat do not further develop, and (ii) parthenocarpy, where ovaries develop into berries without ovule fertilization [16]. So far, grape seedlessness has attracted interest especially for fresh consumption of the so-called table grapes and for producing raisins.

In the case of stenospermocarpy in the Sultanina cultivar, the major causal factor has been identified in a single nucleotide missense mutation in the *VviAGL11* gene [17]. The *VviAGL11* mechanism of action has been hypothesized accordingly [18]. Additional genes have been proposed as regulators of the timing of the arrest of seed development, in a polygenic model in which the *VviAGL11* mutation is necessary for stenospermocarpy and the quantitative variation in the amount of seed traces is controlled by additive effects at other loci [19, 20]. Conversely, the genetic basis of parthenocarpy has not been clarified yet. On the one hand, the very low number of genotypes in which parthenocarpy manifests hampered the study of the trait using association mapping. On the other hand, the nearly complete female and male sterility of parthenocarpic varieties prevents the generation of segregating progenies and the study of the trait using linkage mapping. This type of seedlessness is mainly observed in a small group of genetically unrelated *Vitis vinifera* L. cultivars that have been given similar names like Black Corinth or 'Black Currant' (synonyms of Korinthiaki), White/Red Corinth, Cape Currant and Corinto Bianco and, in which, different reproductive defects affecting ovules, embryo sacs and pollen were reported [21–23].

Parthenocarpy was also identified as the main physiological mechanism leading to seedlessness in a seedless somatic variant of Sangiovese, the Italy's most cultivated winegrape. The identity of the seedless mutant was first discovered from vines occasionally grown in Calabria, in the Southernmost tip of the Italian peninsula, under the name of Corinto Nero. The genotype of those plants matched the one of the Corinto Nero grapevines traditionally cultivated on the Aeolian Islands, off Sicilian shores in Insular Italy, thereby used once for raisins and more recently with other varietals for blending the Malvasia delle Lipari PDO wine [24–26]. Viticulture on the volcanic archipelago of the Aeolian Islands extends over

a mere 150-hectare vineyard area, and Corinto Nero is planted only on a minority of this vineyard. While the current relevance of Corinto Nero for the wine industry is that limited in comparison with seeded clones of Sangiovese, it represents an ideal model for the genetic analysis of parthenocarpy. Our previous pollination trials gave clues to claim both male and female sterility as responsible for a nearly total inability of Corinto Nero to produce seeds. Later, we confirmed male sterility by in vitro pollen viability and germination tests. The genetic analysis of seedlings, which occasionally derived from viable seeds that develop in about 2% of Corinto Nero berries, revealed that the few functional gametes produced by this genotype are mostly unreduced [27]. Accordingly, parthenocarpy seems to be obligatory in Corinto Nero due to pollen and/or embryo sac defects, and both events may arise from meiotic anomalies. Cytohistological studies of megasporogenesis and megagametogenesis, which were previously done only in the seeded Sangiovese [28], need to extend to Corinto Nero for investigating possible abnormalities in the seedless mutant, which is one objective of the present paper. Sangiovese itself seems to have a genetic predisposition to facultative parthenocarpy. If the anthers are manually removed from the flowers prior to pollen release and the emasculated inflorescences are bagged until the end of the flowering period, thereby preventing self-pollination and cross-pollination, Sangiovese can produce a few parthenocarpic berries [27]. Histological studies suggested, however, that megasporogenesis and megagametogenesis occur normally in Sangiovese as well as the formation of a fully developed embryo sac at the onset of anthesis. Those observations nonetheless highlighted the occurrence of some tricarpellate flowers, i.e. developing an ovary with three locules with two ovules each, instead of the typical bicarpellate flowers with two locules [28], which signals the existence of some inherent disorders in flower development.

The extent of this genetic predisposition to flower development disorders in the grapevine germplasm is largely unknown. The molecular bases of parthenocarpy were studied only in natural seedless variants of Sangiovese [27, 29] and Pedro Ximenes [23]. As to causative genetic variation, these investigations focused on SNPs and InDels using available RNA-Seq data in pairwise comparisons between one seeded line and one seedless line. A comparative study of gametogenesis, gene expression and genetic variation was also conducted using a mutant of the line ARI 516, in which parthenocarpy was induced by gamma irradiation [30].

The aims of the present study were to further elucidate anatomical and genetic alterations in Corinto Nero that are associated with the parthenocarpic phenotype. To this end, a comparative histological study was carried out between the female gametophyte in Sangiovese and in Corinto Nero, which showed a lagged megasporogenesis and the arrest of the female gametophyte development at early stages of megagametogenesis in the seedless mutant. A comparative genomic analysis was performed between Corinto Nero and ten seeded Sangiovese clones, which generated a list of functional candidate genes related to cell cycle, meiosis and mitosis with putative sequence variation.

Methods

Plant materials

A commercially available clone of Sangiovese identified by the code R24 (hereafter R24) was used as the reference seeded type for the histological study. The accession of Corinto Nero (hereafter CN) was the same as described in [29] and [27] and corresponds to the VIVC 24403 variety number, www.vivc.de. Inflorescences were sampled from 4-year-old vines of CN and R24 grown in the experimental field "Giaroni" (46.183787N, 11.118893E) of the Fondazione Edmund Mach in San Michele all'Adige (Trento, Italy. FAO Institute code: ITA362). All vines were grown vertically using trellis and according to a Guyot training system. DNA sequences were obtained from ten commercially available seeded clones of Sangiovese (hereafter SG), identified by the codes R10, R24, VCR5, VCR23, VCR30, VCR103, VCR106, VCR207, VCR218 and VCR235. Vines of these proprietary clones were maintained in nursery mother blocks at Vivai Cooperativi Rauscedo, San Giorgio della Richinvelda (Italy; 46.061193N, 12.839853E).

Comparative histological study of the female gametophyte

Flower samples were collected in the 2018 season from young plants of R24 and CN. Growth stages at the sampling dates were expressed according to the modified Eichhnorn-Lorenz (E-L) system [31]. Plant material was sampled from the same inflorescence every 2–3 days starting at stage E-L15 (eight expanding leaves, rapidly elongating shoot, individual adjacent flowers forming compact branches on the inflorescence; reached on May 9.th, 2018) to E-L26 (cap-fall complete; Supplementary Material 1). Branches of the inflorescence carrying from six to ten flowers were collected at each phenological stage, immediately fixed in FAA (10:50:5:35 of 37% formaldehyde: 95% ethanol: acetic acid: distilled water) and processed by sectioning and staining with a safranin O-fast green FCF staining combination according to the protocol described by [28]. Then, 3–7 µm thick sections were obtained using an automated rotary microtome (Leica RM2247) and examined in bright field using a Leica DM500 microscope equipped with a Leica ICC50 HD camera (Leica Microsystems, Germany). LAS EZ version 3.4.0 imaging software (Leica Microsystems, Germany) for "live" imaging observations was used to

capture Digital images and annotations were taken using the LAS EZ version 3.4.0 software (Leica Microsystems, Germany). Image post-processing, which consisted in enhancing contrast and sharpness, was performed using ImageJ software [32]

Analysis of genomic diversity between Corinto Nero and ten different seeded clones of Sangiovese

Whole genome resequencing

DNA was extracted from young leaves. DNA of CN was isolated using the DNeasy Plant Mini kit (QIAGEN, USA) with RNase treatment and according to the manufacturer's instructions. Before the identity of CN as a SG mutant was disclosed, the other 10 Sangiovese clones had been sequenced for different purposes. DNA of 8 SG clones was isolated following a CTAB-based protocol [33]. DNA of R24 and VCR23 clones was isolated following the same CTAB-based protocol but with a preliminary step of nuclei isolation to reduce the contribution of cytoplasmic DNA. DNA quality was checked using a Nanodrop 8000 spectrophotometer (Thermo Fisher Scientific, DE, USA), and on a 1% agarose gel by electrophoresis. DNA was quantified using a Synergy fluorimeter (Agilent Technologies, Waldbronn, Germany). DNA fragmentation and library preparation were performed according to standard Illumina protocols. Paired-end sequencing was performed with Illumina Genome Analyzer II (GAII) (2 × 75 bp), Illumina HiSeq 2000 (2 × 100 bp) and Illumina Hiseq 2500 (2 × 125 bp) sequencers as described by [34]. Raw reads were processed for adapter removal, quality trimming and filtering for organelle DNA with erne-filter algorithm version 1.4 (https://erne.sourceforge.net). Post-processed paired-end reads longer than 50 bp were aligned to the PN40024 12X.0 grapevine reference genome using the BWA-mem algorithm, with default parameters (https://bio-bwa.sourceforge.net/bwa.shtml). To reduce false positives, PCR duplicates were removed using MarkDuplicates from Picard tools (http://broadinstitute.github.io/picard/). Local realignment around InDels was performed with the RealignerTargetCreator and IndelRealigner tools of the GATKv2.0 (https://gatk.broadinstitute.org/hc/en-us). Reads with a mapping quality > 10 were retained.

Analysis of genomic variation

SNPs and InDels shorter than 50 bp were identified using GATK UnifiedGenotyper [35] with default parameters, except that heterozygosity was set to 0.01. Raw Single Nucleotide Variants (SNVs) were retained if biallelic, with a coverage > 15 ×, invariant in other *V. vinifera* cultivars, not residing in repetitive regions, with allele frequency > 0.10, with < 55% of missing data. Private variants in CN were retained for further analysis. SNP annotation was performed using Annovar with the V2.1 gene prediction [36].

Different types of SVs were identified with the following approaches. Deletions were called using DELLY [37], only if the alternative genotype was invariable among the ten seeded SG clones and different from CN. TE insertions were identified by paired-end mapping (PEM), which uses deviation from the expected span size and/or orientation of mapped paired-end reads [38]. Reads that span the insertion breakpoint were quantified to call the genotypes for the structural variant. The following thresholds were used for assigning the genotype: ratio ≤ 0.25 = absence of insertion (0/0), 0.25 < ratio ≤ 0.75 = insertion likely heterozygous (0/1) and ratio > 0.75 = insertion likely homozygous (1/1). The presence of mosaic structural variation (MSV) and chromosomal aberrations was investigated using the reduction of heterozygosity (ROH) signal and the χ-scan software, as described by [39] and [40]. In this approach, allele read coverage ratios are compared between any two pairs of clones as a proxy for the presence of ROH and this is combined with the information of local read coverage.

A Circos plot containing all SVs identified in the comparative analysis was drawn using ShinyCircos v.2.0 [41].

Genomic data analysis

The *V. vinifera* 12X reference genome release 52 annotation available at the EnsemblPlants platform [42] was used for gene annotation in the chromosomal regions where putative structural variation was identified (deletions, insertions of TEs and MSV). Gene functional categories were defined according to The Gene Ontology Resource [43, 44], UniProt database [45], as well as using the grape reference gene catalog [46] where the corresponding gene IDs in the 12X.v2 grapevine reference genome assembly and their annotations (VCost.v3) were available [47]. Gene expression data in SG and CN were retrieved from [29]. Candidate genes were also checked for co-localization with known QTLs for fertility, seed content and berry size as reported in [48]. QTLs were projected onto a consensus genetic map anchored to the 12X.v2 grapevine reference genome assembly [48].

SNP validation and quantitative RT-PCR expression analysis

The candidate gene *VIT_05s0020g04170* (*DMC1*), carrying a C > T SNP at the chromosomal position chr5:5,814,092, was selected for further exploration, considering its predicted function and its putative role in Arabidopsis [49, 50]. The presence of the *DMC1* SNP variant was validated through PCR amplification and Sanger sequencing of genomic DNA from young leaves of the two Sangiovese clones (R24 and CN) and of Pinot Noir as a control. Primers were designed using

Primer3Plus [51] and the 12X.v2 version of the reference genome sequence. Primer sequences are reported in Supplementary Material 2. PCR products were purified using the Eurosap PCR Enzymatic clean-up kit (Euroclone S.p.A, MI, Italy). Sequencing reactions were performed using the same primers as in the PCR and then sequenced by capillary electrophoresis using an ABI 3730xl DNA Analyzer. Chromatograms were aligned using the MEGA6 software [52] and visually inspected using BioEdit v7.2.0 [53]. The CD-Search tool available on the NCBI portal was used to check whether mutations affected conserved sites or domains. Quantitative RT-PCR analysis was performed at ten different phenological stages (Supplementary Materials 1 and 2). A T-student test was performed using PAST version 3.14 to test the statistical significance of the differences between R24 and CN at each phenological stage ($p < 0.05$).

Results

Comparative histological study of the female gametophyte

The R24 seeded clone and CN bloomed 19 and 21 days, respectively, after the first sampling date (stage E-L15). Sampling was performed from E-L15 stage to E-L26 stage. Detailed description of the developmental status of the female gametophyte at each phenological stage for each clone is reported in Supplementary Material 3. Figure 1 summarizes the match between each step of female gametophyte development and the phenological stages studied in the two clones.

Stage E-L15

The development of the female gametophyte in CN was similar to the one of the seeded R24 clone (Fig. 2A and B; Supplementary Material 3). However, while a compact nucellus was consistently observed in all ovules in R24, it appeared less compact presenting some intercellular spaces in CN (Supplementary Material 4).

Stage E-L15 + 2

No significant changes were observed in R24 regarding the development of the integuments and nucellus, with anatropy progressing normally. In contrast, anatropy in CN was at a very early stage in all ovules of one sample, while in the other one all ovules were almost completely anatropous. Additionally, slight differences in integuments development were observed between samples (Supplementary Material 3). The megaspore mother cell (MMC) was identified at various substages of prophase I of meiosis in nearly all the examined ovules of both clones (Fig. 2C and D, Supplementary Materials 3, 5 and 6).

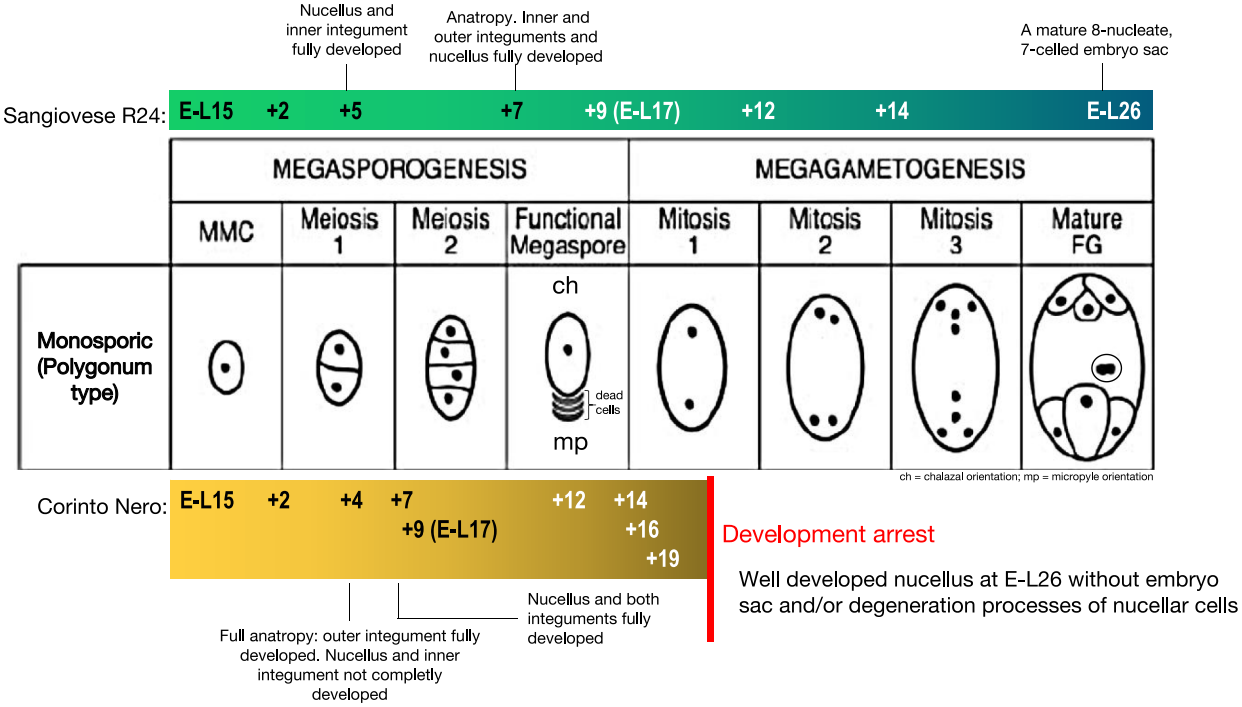

Fig. 1 Modified Fig. 2 from Yadegari & Drews 2004 (http://doi.org/10.1105/tpc.018192). Schematic representation of the match between each step of female gametophyte development according to the histological observations and the phenological stages analyzed in Sangiovese R24 and Corinto Nero. Phenological stages in days after the beginning of the sampling at E-L15: + 2, + 5 (+ 4 in Corinto Nero), + 7, + 9 (E-L17), + 12, + 14, + 16, + 19 and E-L26 (flowering)

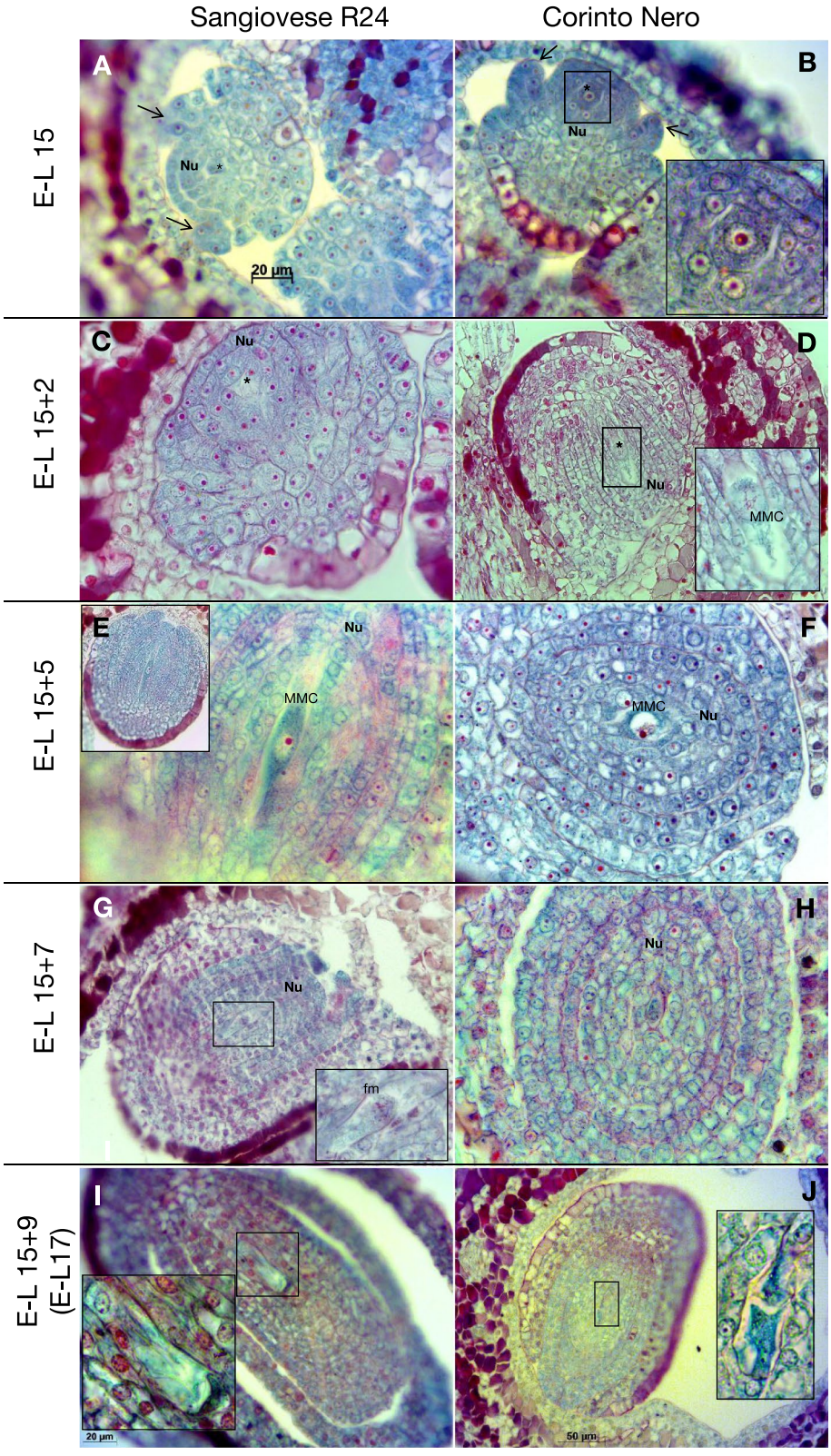

Fig. 2 (See legend on next page.)

(See figure on previous page.)

Fig. 2 Developing female gametophyte from phenological stage E-L15 to E-L15 + 9 (= E-L17) in the Sangiovese R24 seeded clone (R24) and the seedless mutant Corinto Nero (CN). Safranin O—fast green FCF staining combination stains with cyan/green hues the cytoplasmatic component of the cells while nuclei and nucleoli stain in reddish/magenta. Stage E-L15: in all the investigated ovules of both clones the beginning of the nucellus was observed, with nucellar cells in different stages of mitosis, as well as lateral bosses indicating the initiation of the inner integument (black arrows; **A**, **B**). Cells undergoing periclinal divisions at the base of the inner integument were visualized, which likely points to an initial formation of the outer integument with larger rectangular cells. In most of the ovules of both clones it was observed a centrally located, enlarged cell with dense cytoplasm and prominent nucleus, that was going to be the MMC (megaspore mother cell, *). Stage E-L15 + 2: central MMC (*) in early stages of prophase I of meiosis in both clones (**C**, **D**). Stage E-L15 + 5 in **E** (E-L15 + 4 in CN, **F**): MMC in early stages of meiosis I. Stage E-L15 + 7: a functional megaspore (fm) is already visible in R24 which indicates the end of megasporogenesis (**G**); in CN the beginning of prophase II of meiosis is undergoing, two cells are visible (**H**). Stage E-L15 + 9 (= E-L17): in R24 the functional megaspore is entering megagametogenesis with the onset of mitosis I and megaspores appear as dead cells in the micropylar end (**I**). In CN, two cells in prophase II of meiosis are visible, it is still in megasporogenesis (**J**). Nu = nucellus. Magnifications: 400 × in **A**, **B**, **I**, **J**; 800 × in **D**, ovule overview in **E**, **G**; 1000 × in details in **B**, **I** and **J**; 2000 × in **C**, **E**, **F**, **H** and details in **D** and **G**

Stage E-L15 + 5 (E-L15 + 4 in CN)

The MMC was observed in different stages of meiosis I in the examined ovules of both clones (Fig. 2E and F, Supplementary Material 7). However, while R24 presented a compact and well-developed nucellus, CN did not show yet a fully formed nucellus. Slight differences in the degree of integument development were also observed between R24 and CN. Additionally, a small triangular empty space between nucellus and inner integument towards the micropylar end, called endostome, was observed in several ovules of the seeded R24. The endostome was larger and present in most of the ovules of CN (Supplementary Materials 3 and 8 A).

Stage E-L15 + 7

All analyzed ovules of CN were completely anatropous at this stage (Supplementary Material 8B) with both integuments and nucellus fully and normally developed, as in seeded R24 (Fig. 2G and H, Supplementary Material 3). However, while R24 displayed a linear tetrad arrangement consisting of the functional megaspore at the chalazal pole and three degenerated megaspores at the micropylar end following MMC meiosis (megasporogenesis; Supplementary Material 9), CN showed that megasporogenesis was still ongoing in most of the examined ovules, specifically in the early prophase of the second meiotic division (Supplementary Material 10).

Stage E-L15 + 9 (= E-L17)

All examined ovules of both clones were fully anatropous, with normally developed nucellus and integuments. Megasporogenesis had been completed in R24 by this stage. On the contrary, this process was delayed or slowed, and still ongoing at this stage in CN (Fig. 2I and J, Supplementary Material 3).

Stages E-L15 + 12 until E-L26 (anthesis)

No substantial changes were observed in R24 samples regarding the integuments and nucellus cells at the successive phenological stages analyzed (E-L15 + 12, E-L15 + 14 and E-L26). However, notable developments were detected in the transformation of the functional megaspore into the mature embryo sac, which was fully formed by the time of flowering. In some cases, early signs that are indicative of the beginning of fertilization were also observed (Fig. 3A, C, E and G, Supplementary Materials 3 and 11—13).

In the samples from CN at stage E-L15 + 12, all the examined ovules were well-developed and a functional megaspore was observed in most of them along with remains of the other three remaining megaspores that had died out (Fig. 3B, Supplementary Materials 14–16). By stage E-L15 + 14 all analyzed ovules were fully and normally developed, but the functional megaspore was observed only in a couple of them at the prophase of mitosis I (Fig. 3D and F, Supplementary Material 17). However, at stage E-L15 + 16, despite the presence of a well-developed nucellus, the characteristic cell types of the embryo sac were absent from most of the ovules, with only a functional megaspore undergoing mitosis I. Traces of degenerated megaspores were observed in a single ovule (Supplementary Materials 18–19). At the last stage of observation before flowering (E-L15 + 19), a binuclear embryo sac was observed in one ovule and a clearly defined embryo sac containing two synergids and the outline of the egg cell were present at the micropylar end in another ovule. However, degeneration processes from the center of the nucellus (dead nucellar cells) and traces of dead megaspores were observed in all other ovules examined (Supplementary Material 20). At flowering (E-L26), although all the analyzed ovules initially displayed a normal development, no embryo sac was detected in the well-developed nucellus. Instead, we observed ongoing processes of degeneration in the central nucellar cells and/or traces of dead megaspores at the chalazal end (Fig. 3H, Supplementary Material 3).

According to these histological observations, megasporogenesis (i.e. development of a functional megaspore from the MMC through two consecutive meiotic divisions) lasted around 7 days in R24, from stage E-L15 to stage E-L15 + 7. The second meiotic division likely progressed faster than the first one, since only processes of the first meiotic division were observed until stage E-L15 + 5. Subsequently, megagametogenesis (i.e.

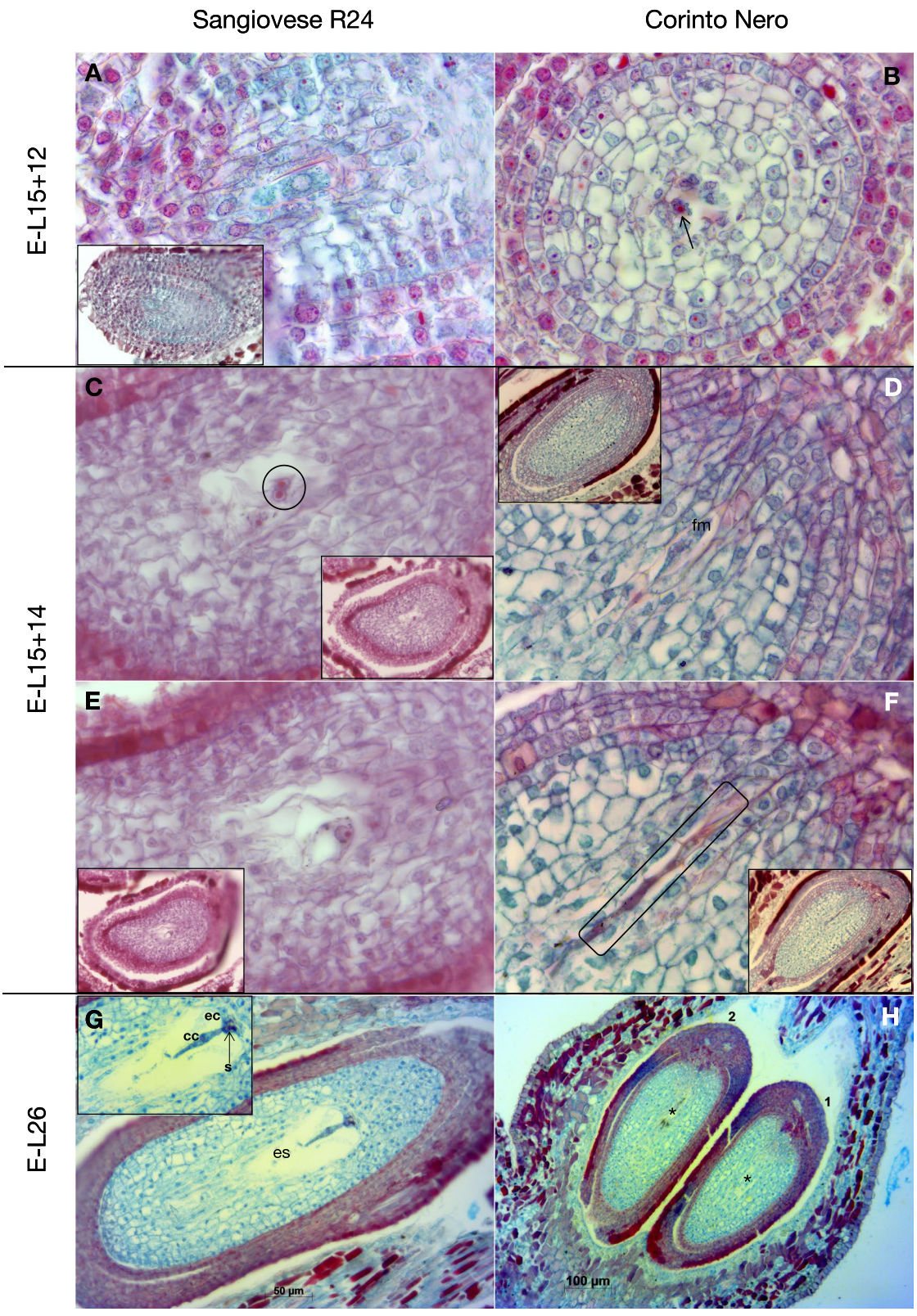

Fig. 3 (See legend on next page.)

(See figure on previous page.)

Fig. 3 Developing female gametophyte from phenological stage E-L15 + 12 to flowering (E-L26) in the Sangiovese R24 seeded clone (R24) and the seedless mutant Corinto Nero (CN). E-L15 + 12: start of mitosis II (megagametogenesis) in R24 (**A**), while in CN the functional megaspore (indicated by the arrow) with a red nucleus is visible as well as traces of dead megaspores (dark purple cells to the right of the functional megaspore) which corresponds to the end of megasporogenesis; **B**). E-L15 + 14: two nuclei (circle) of 4-nucleate embryo sac (which develops after mitosis II) with cytoplasmatic strands connecting each pair of nuclei in the chalazal and micropylar poles and between opposite poles are visible in R24 (**C**, **E**); in CN the functional megaspore (fm) is in the prophase of mitosis I in **D**, while in **F** fragments of dead megaspores (rectangle) are observed, without any cells or nuclei of a developing embryo sac. E-L26 (flowering): ovule with normal embryo sac (es) structures: visible central cell (cc), egg cell contour (ec) and degradation signs of the synergids (s) in R24 (**G**); two well developed ovules of CN without embryo sac and with initial degeneration signs in the center of the nucellus (*) and integuments (**H**). Magnifications: 2000 × in **A**—**F**, 100 × detail in **G**, 400 × in **G** and 200 × in **H**

development of the functional megaspore into a mature embryo sac through three consecutive mitoses by monosporic polygonum-type) was observed to occur from stage E-L15 + 9 until flowering (E-L17) over an interval of at least 9–10 days (Fig. 2, Supplementary Material 3). In contrast, histological analysis in CN revealed not only a lag in the development of the nucellus relative to the integuments during early stages, but also a significantly slower progression of megasporogenesis. More specifically, megasporogenesis took approximately 12 days to complete, due to a prolonged second meiotic division in comparison with the seeded clone. Even in cases where a functional megaspore was produced, its further development into a mature embryo sac was arrested at early stages of megagametogenesis (Figs. 1 and 3).

The majority of flowers from R24 presented a bicarpellate, syncarpous ovary (i.e. fused carpels into a unified compound gynoecium) divided into two locules with two ovules each, resulting in a total of four ovules per flower. However, in four out of the 20 analyzed flowers a tricarpellate, syncarpous ovary was observed, consisting of three locules with two normally and fully developed ovules in each one and, thus, with a total number of six ovules per flower (Fig. 4A and C, Supplementary Material 3). Unlike R24, all 23 analyzed flowers from CN displayed a bicarpellate, syncarpous ovary (Fig. 4B).

Comparative genomic analysis between Corinto Nero and ten seeded clones of Sangiovese

Identification of private SNPs and InDels

A total of 2,542 putative variant sites were called in CN potentially carrying novel and monoallelic mutations (Fig. 5, track 1). Among these, 151 were in exons and one affected a splicing site (Tables 1 and 2 and Supplementary Material 21). Gene ontology (GO) annotations under the Biological Processes (BP) category (Supplementary Material 22) allowed the functional classification of 119 out of 204 genes overlapping splicing and non-synonymous exonic SNPs (Tables 1 and 2). The remaining genes included 69 unclassified ones and 16 with unmapped IDs. All 119 classified genes were distributed accross ten BP-GO main categories (Fig. 6). For complete and detailed information about all genes within each category see Supplementary Material 21.

A total of 1,038 putative heterozygous InDels were called in CN. In 24.9% of cases, the seeded SG clones were homozygous for the reference allele (with no more than 2 missing data among samples); while in the remaining 75.1% of cases, the seeded SG clones were homozygous alternative with respect to the reference (Table 1). Three putative InDels were in exonic regions. All of them were frameshift mutations (*VIT_15s0024g00700*, *VIT_15s0048g00910* and *VIT_00s2376g00010*. Figure 5 track 2, Table 1 and Supplementary Material 23).

Larger deletions

A total of 92 signals of variation in depth of coverage were identified, potentially suggesting differences in deletion events between CN and SG seeded clones (Fig. 5, track 3 and Table 3). These signals range in size from 422 to 1,274 bp (Supplementary Material 24). CN was heterozygous for two putative deletions (chr1:15,298,475–15,299,482 and chr12:21,896,319–21,896,741), but in both cases all SG seeded clones were homozygous for the deletion with respect to the reference genome. As reliable somatic mutations are expected to be monoallelic and novel, these events represent weak candidates for explaining the CN phenotype. These putative deletions did not overlap with any predicted gene (Supplementary Material 24).

Insertions of transposable elements (TE)

A total of 433 discordant paired-end mapping signals were detected, suggesting putative insertions of transposable elements (Fig. 5 links in the innermost circle, Table 4). However, the CN genotype differed from the reference genome for only 358 of them. Of these, 210 signals were classified as heterozygous and novel in CN and absent from SG seeded clones and from the reference genome. In these genomic regions, 37 genes were predicted, but only a few of them were associated with a strong reliable signal for the insertion (Supplementary Materials 25 and 26); for instance, *VIT_01s0182g00020*, *VIT_10s0092g00470*, *VIT_19s0093g00140* are involved in regulation of transcription and protein phosphorylation, and *VIT_09s0002g03350* codes for an uncharacterized protein. The other 148 signals were classified as homozygous in CN and heterozygous in SG seeded clones. In 38 of the cases, the signals overlapped with 35 predicted

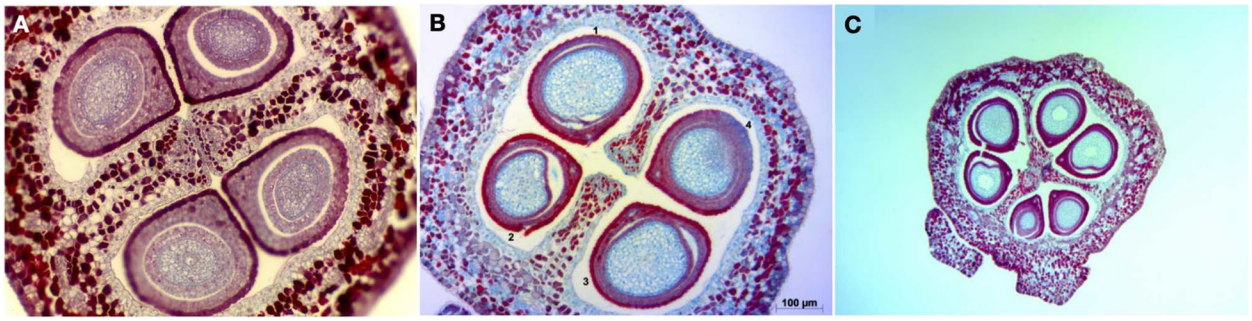

Fig. 4 Bicarpellate, syncarpous ovaries divided into two locules with two ovules each in flowers of Sangiovese R24 (**A**) and in Corinto Nero (**B**). Tricarpellate syncarpous ovary divided into three locules with two ovules each observed in four out of the 20 analyzed flowers of Sangiovese R24 (**C**)

gene models. The genes associated with the strongest signals of putative insertion were: *VIT_09s0070g00010*, *VIT_04s0023g03320* (involved in plant-type cell wall modification processes), *VIT_02s0025g03090*, *VIT_15s0046g01170*, *VIT_16s0022g00820*, *VIT_17s0119g00030* (involved in signal transduction), *VIT_02s0012g00190* (involved in cellular component organization processes), *VIT_05s0020g02220*, *VIT_15s0046g03670* (tagged with pyruvate and malate metabolic processes), *VIT_07s0205g00140* (involved in mitotic sister chromatid segregation, microtubule-based movement, microtubule depolymerization) and *VIT_09s0002g00020* (related to cell cycle, cell division, homologous recombination and mitotic sister chromatid cohesion; Supplementary Materials 25 and 27).

Search for mosaic structural variants (MSV) and chromosomal aberrations

No significant ROH signal was detected in the comparison between CN and seeded SG clones, which excludes the occurrence of large deletions and/or duplications and chromosome replacements in CN (Supplementary Material 28, Fig. 5 track 4). However, small regions where the signal exceeds the threshold of statistical significance for all ten SG clones were detected (Supplementary Material 28). If present in homozygous or hemizygous regions, MSV would have gone undetected using this approach. We could exclude that CN is affected by aneuploidies, but we cannot exclude from short-read sequencing data that CN is affected by translocations not resulting into evident copy number variation.

Genomic variation in genes

A total of 403 genes overlapped with putative SNPs (Table 2 and Supplementary Material 21), InDels (Table 1 and Supplementary Material 23) or structural variation (deletions in Supplementary Material 24; TE insertions in Supplementary Material 25) between CN and the SG seeded clones (Fig. 7). Of these, 32 were in the confidence intervals of previously reported QTLs for fertility, seed content and berry size, as reported by Delfino et al. 2019 (Supplementary Material 29).

DMC1 analysis

Among the candidate genes with annotated functions related to cell cycle, the gene *VIT_05s0020g04170*, a DNA recombinase *RecA/Rad51/DMC1* homolog, was chosen for further investigation. First, the C > T nucleotide substitution at the chromosomal position chr5:5,814,092 in CN, was experimentally validated by amplicon sequencing in R24 and CN (Supplementary Material 30). This is a non-synonymous substitution that causes an amino acid change in the predicted protein (Supplementary Material 21). According to the tools VEP and CD-Search, this R173Q amino acid substitution is predicted to have a moderate impact on the protein structure, but it is located within a conserved domain (P-loop NTPase and PLN03187 domain superfamilies). Then, the *DMC1* expression profile was analyzed in both clones at ten different phenological stages from the earliest development of the inflorescence to pepper-corn sized berries (Fig. 8). *DMC1* expression level notably increased at stage E-L14 in both clones, although it was lower in CN. However, statistically significant differences were detected only at stage E-L15, prior to the start of megasporogenesis (as evidenced by the histological analysis, see above), and at the stage E-L26 (anthesis) at the time that mature embryo sacs have already formed in the seeded clone.

Discussion

Early arrest of female gametophyte development in Corinto Nero ovules

Prior to the present study, seedlessness in CN was thought to be caused by pollen and/or embryo sac defects likely arising from meiotic anomalies. Indeed, the rare functional gametes that are produced by CN are predominantly unreduced, mainly diploid, which suggests they arise through apomeiosis (suppressed or imperfect meiosis) [27]. The histological analysis of the female gametophyte reported in the present work supports this hypothesis, revealing an altered megasporogenesis in CN

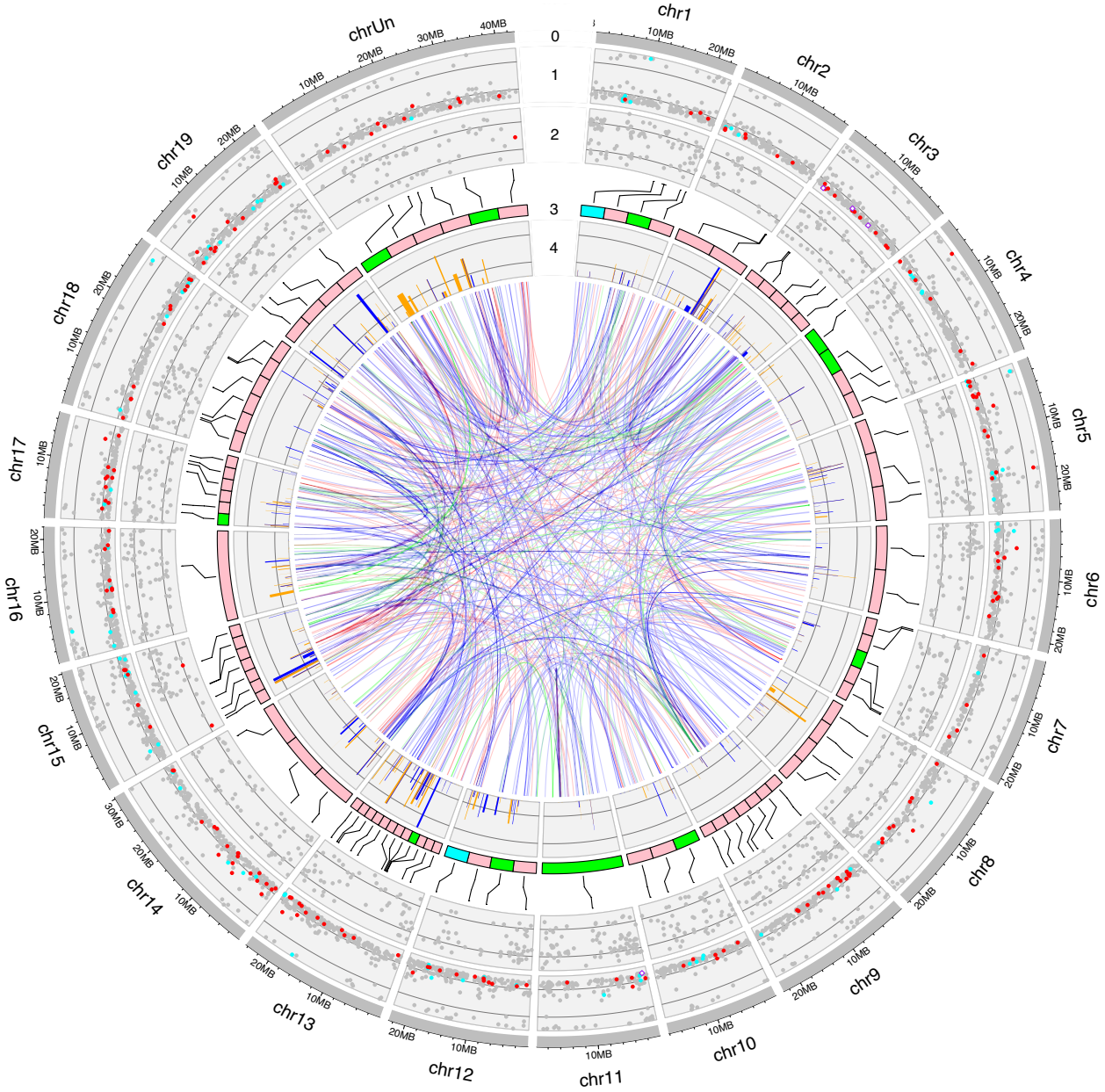

Fig. 5 Distribution of genomic variation in the seedless mutant Corinto Nero (CN) in comparison with ten Sangiovese seeded clones (SG). Track 1: heterozygous SNPs. In grey 4047 non-exonic SNPs (3740 of them private for CN), in red 192 non-synonymous ones (all private SNPs in CN except three), in purple 4 private splicing SNPs and in cyan 81 synonymous ones (all private except 5 of them); y axes: allele frequency 0–1, dark lines at 0.25 and 0.75. Track 2: InDels. Red dots indicate the three ones located in exonic regions (y axes: allele frequency 0–1, dark lines at 0.25 and 0.75). Track 3: Deletions. No private deletions for CN were detected, but heterozygous in CN and homozygous alternative in SG (cyan), absent in CN (homozygous reference) and heterozygous in SG (pink) or absent in CN and homozygous alternative in SG (green). Track 4: mosaic structural variation (MSV). Reduction of heterozygosity (ROH) signal is statistically significant in CN (orange) and in SG seeded clones (blue); y axes indicate the number of seeded clones for which the signal was consistent, 1–10. Links: TE insertions. Red for heterozygous events in CN and homozygous reference state in SG, blue for homozygous alternative events in CN and heterozygous state in SG and green for homozygous reference state in CN and heterozygous event in SG

compared to SG. Specifically, CN exhibits a disrupted meiotic progression with an extended second meiotic division, ultimately leading to the arrest of the female gametophyte development at the early stages of megagametogenesis (Figs. 1 and 3). These findings indicate that failure of ovule development in CN likely occurs during or shortly after megasporogenesis. This pattern aligns with observations in Corinto Bianco and Black Corinth, where the formation of integuments and nucellus starts normally, but their development ceases past the formation of the megaspore or the degeneration of the embryo sac. In contrast, ovule development in other

Table 1 Total number of SNPs and InDels detected, after filtering criteria, in Corinto Nero classified according to the variant function and distribution according to the genotype of the studied clones: CN|XX = Corinto Nero genotype, SG_X|XX = Sangiovese seeded clones genotype, subindex indicates the number of Sangiovese seeded clones that presented that genotype ("00" = homozygous as in the reference genome PN40024 12X.0, "01" = heterozygous variant, "11" = homozygous variant)

Variant function	Number		Percentage		CN|01—SG_{10}|00		CN|01—SG_9|00		CN|01—SG_8|00		CN|01—SG_{10}|11		CN|01—SG_9|11		CN|01—SG_8|11	
	SNPs	Indels	SNPs	Indels	SNPs	Indels	SNPs	Indels	SNPs	Indels	SNPs	Indels	SNPs	Indels	SNPs	Indels
Up- & downstream	700	194	15.5%	18.7%	404	35	175	10	56	6	57	125	7	17	1	1
Exonic	282	3	6.3%	0.3%	151	1	87	0	35	1	8	1	1	0	0	0
Intergenic	2465	459	54.6%	44.2%	1334	81	655	26	283	8	159	311	29	26	5	7
Intronic	923	342	20.5%	32.9%	567	56	220	19	84	5	46	249	6	12	0	1
Splicing	4	0	0.1%	0.0%	1	0	3	0	0	0	0	0	0	0	0	0
UTR3'	90	30	2.0%	2.9%	58	5	22	2	7	1	1	21	0	1	2	0
UTR5'	49	10	1.1%	1.0%	27	2	18	0	2	0	1	7	1	1	0	0
TOTAL	4,513	1,038	100%	100%	2,542	180	1,180	57	467	21	272	714	44	57	8	9

parthenocarpic cultivars such as White Aspirant, Red Corinth and White Corinth ceases at an earlier stage, most commonly before anatropy is established, and ovules may possess only a single integument [22, 23].

Candidate genes for the Corinto Nero seedless phenotype

In this work, we identified a few thousand putative private variants of different types in Corinto Nero in the portion of the genome that is explorable using a resequencing approach and short-read alignments against a reference genome assembly. Defective meiosis during the development of male and female gametophytes in CN is thought to play a key role in seedlessness. DNA mismatch repair, sister chromatid cohesion, homologous chromosome pairing, inter-homolog recombination and chromosome segregation are essential processes during meiosis. More specifically, failure in chromosome segregation might explain the formation of imbalanced gametes [54]. Most of the candidate genes discussed hereafter may affect these processes.

DMC1 ("Disrupted Meiotic cDNA1")

DMC1 has a crucial and conserved role in meiosis in sexual organisms [55], as it encodes a protein promoting inter-homolog recombination, which is an essential step for bivalent formation and correct partition of chromosomes during the first division of meiosis. In different plant species, like Arabidopsis, barley, chrysanthemum and rice, a sterility phenotype was correlated with the unbalanced segregation observed during both male and female meiosis in *dmc1* mutants. Irregularly shaped and heterogeneously sized microspores were noted in *dmc1* anthers, which reflects variable chromosomal DNA content, and the development of megaspore mother cell was found to arrest just after meiosis or at the early stage of megagametogenesis [50, 56–59]. Similar functional and morphological anomalies have been observed in CN gametes. *DMC1* was also suggested to affect diplospory [60], which is the same mechanism proposed for the formation of CN unreduced gametes. The heterozygous C > T SNP variant that we found to affect the grapevine *DMC1* homolog gene in CN is present in a conserved protein domain [58, 61–65]. As hypothesized for Corinto Bianco [23], CN might also be a somatic mutant with a dominant heterozygous mutation. Similarly, the mutation affecting *DMC1* in a barley mutant was found to exhibit semi-dominance [57]. In other plant species the *DMC1* gene was reported to be strongly expressed in meiocytes in reproductive organs (pollen mother cells and MMC), with elevated levels observed during prophase I when meiotic recombination occurs, and *DMC1* proteins were found on leptotene and zygotene chromosomes [49, 57, 64, 66–68]. A significantly lower expression of *DMC1* gene was observed in CN with respect to R24, when the

Table 2 Number of SNPs in Corinto Nero overlapping exonic regions classified according to the type of variant and distribution of the exonic variants according to the genotype: CN|XX = Corinto Nero genotype, SG_X|XX = Sangiovese seeded clones genotype, subindex indicates the number of seeded clones that presented that genotype ("00" = homozygous as in the reference genome PN40024 12X.0, "01" = heterozygous variant, "11" = homozygous variant)

Variant type	Number	Percentage	CN|01—SG_{10}|00	CN|01—SG_9|00	CN|01—SG_8|00	CN|01—SG_{10}|11	CN|01—SG_9|11
Synonymous	82	29.1%	50	14	13	5	0
Non-synonymous	185	65.6%	91	68	22	3	1
Stop-gain	14	5.0%	9	5	0	0	0
Stop-loss	1	0.4%	1	0	0	0	0
TOTALE	282	100%	151	87	35	8	1

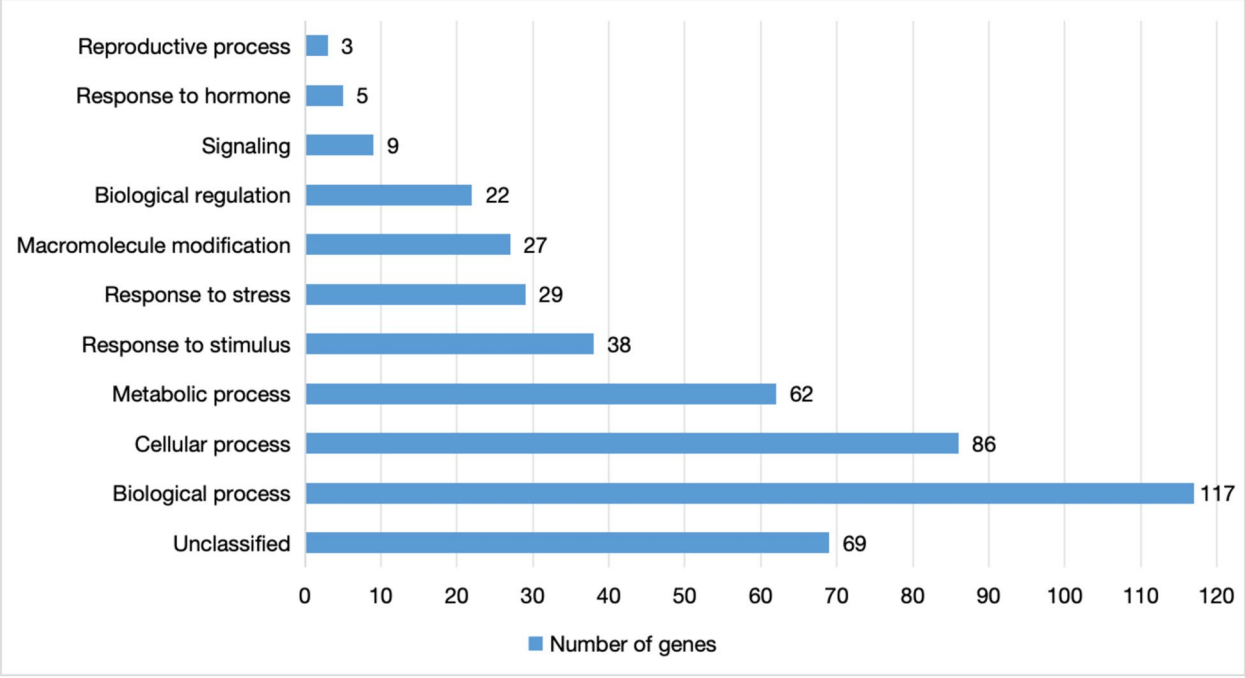

Fig. 6 Number of genes within the main BP-GO categories represented among the list of 204 genes overlapping splicing or non-synonymous, stop-gain and stop-loss exonic SNPs between Corinto Nero and Sangiovese seeded clones

MMC was approaching the onset of the megasporogenesis (Fig. 8). Further investigation is needed to assess if the observed lower expression of *DMC1* in the seedless mutant might be causally associated with the phenotype. However, we did not detect genetic variation in and around this gene in CN that may explain a differential regulation with respect to seeded clones.

Other candidate genes

Besides *DMC1*, we identified other genes that might determine seedlessness in CN (Fig. 6, Supplementary Materials 21, 23, 25, 28, 29). They are discussed below.

VIT_05s0049g02100 (with a T > A SNP chr5:9,734,087 in CN) encodes a predicted protein with similarity to the curly leaf 1-like protein PhCLF1 that is involved in methylation processes. *Petunia hybrida* curly leaf 1 is suggested to be an ortholog of the Arabidopsis *CURLY LEAF* (*CLF*) gene. It is possible that *PhCLF1*, like *CLF*, is involved in the maintenance of transcriptional repression of a class C floral homeotic gene or other unknown target genes [69] that may control floral organ identity. The expression of class C genes in the fourth whorl specifies carpel identity, while its combined expression with class B genes in the third whorl leads to stamen identity.

VIT_09s0002g00020 (with a homozygous TE insertion in CN) encodes a predicted protein with similarity to the *PDS5* (Precocious Dissociation of Sisters 5) cohesion cofactor. The cohesin protein complex is essential for sister chromatid cohesion, ensuring faithful chromosome segregation during mitosis and meiosis, and is also involved in chromosome condensation, gene expression, development, DNA repair and somatic homologous recombination. *PDS5*-like proteins are functional during meiosis, although with particular features in different species [70].

VIT_00s0485g00020 (with a T > C SNP chrUn:30,378,589) is predicted to encode a DNA mismatch repair protein with similarity to *MSH3*. In various

Table 3 Distribution of the deletions detected by DELLY method along chromosomes (Chr) and according to the genotype ("00" = absence of deletion as in reference genome PN40024 12X.0, "01" = heterozygous deletion, "11" = homozygous deletion) of the Sangiovese clones. Deletion was called if the genotype was invariable among the ten seeded Sangiovese clones (SG) and different from the seedless mutant Corinto Nero (CN)

Chr	Nr	Percentage	Number of detected deletions		
			SG|01-CN|00	SG|11-CN|00	SG|11-CN|01
chr1	4	4.35%	2	1	1
chr2	2	2.17%	2	0	0
chr3	5	5.43%	5	0	0
chr4	4	4.35%	2	2	0
chr5	3	3.26%	3	0	0
chr6	2	2.17%	2	0	0
chr7	5	5.43%	4	1	0
chr8	4	4.35%	4	0	0
chr9	7	7.61%	7	0	0
chr10	3	3.26%	2	1	0
chr11	1	1.09%	0	1	0
chr12	4	4.35%	2	1	1
chr12_random	1	1.09%	1	0	0
chr13	12	13.04%	11	1	0
chr13_random	1	1.09%	1	0	0
chr14	3	3.26%	3	0	0
chr15	7	7.61%	7	0	0
chr16	1	1.09%	1	0	0
chr17	6	6.52%	5	1	0
chr17_random	1	1.09%	1	0	0
chr18	6	6.52%	6	0	0
chr19	4	4.35%	4	0	0
chrUn	6	6.52%	4	2	0
TOTALE	92	100.00%	79	11	2

Table 4 Distribution of the TE insertions along chromosomes and according to the genotype of Sangiovese seeded clones and of the seedless mutant Corinto Nero (SG|XX and CN|XX, respectively; "00" = absence of TE insertion, "01" = heterozygous TE insertion, "11" = homozygous TE insertion)

Chromosome	SG|00—CN|01	SG|01—CN|11	SG|01—CN|00	TOTAL
chr1	11	10	4	25
chr2	13	8	7	28
chr3	9	10	3	22
chr4	8	5	1	14
chr5	9	9	4	22
chr6	10	6	2	18
chr7	9	7	4	20
chr7_random	0	1	0	1
chr8	8	2	0	10
chr9	17	10	3	30
chr9_random	0	1	0	1
chr10	6	5	5	16
chr10_random	0	1	0	1
chr11	7	6	2	15
chr11_random	1	0	0	1
chr12	10	9	2	21
chr13	11	4	3	18
chr13_random	1	0	0	1
chr14	9	3	3	15
chr15	3	8	5	16
chr16	10	13	1	24
chr16_random	2	0	0	2
chr17	8	5	4	17
chr17_random	1	1	1	3
chr18	11	13	6	30
chr18_random	1	2	2	5
chr19	14	6	2	22
chrUn	21	3	11	35
TOTAL	210	148	75	433

plants, mismatch repair functions extend well beyond post-replication error correction [71], as certain mismatch repair proteins play positive roles in the promotion of meiosis, including meiotic recombination, and impact on fertility [72, 73]. *VIT_04s0023g03350* and *VIT_06s0004g03800* (affected by a T > C SNP chr4:19,913,828 and a C > T SNP chr6:4,776,574) encode components of *SWR1*(*SWi2/snf2*-Related 1)/*INO80* chromatin remodeling complex, *TRA1a* and *NFRKB1* (nuclear factor kappa-B-binding-like protein 1), respectively. The *SWR1/INO80*-complex plays essential roles in DNA repair, checkpoint regulation, DNA replication, telomere maintenance and chromosome segregation. Interestingly, some core *SWR1/INO80*-complex subunits were shown to act in Arabidopsis female gametophyte development, with a role during meiosis [74, 75]. The chromatin remodeling complex *SWR1* was also suggested to regulate *DMC1* expression [76]. *VIT_16s0022g00230* (with a G > T SNP chr16:11,018,044) is a member of the *SMC2* (*Structural Maintenance of Chromosomes*) gene family. SMC2 and SMC4 are the core subunits of condensin, a complex required for chromosome condensation and segregation. Consistently, defects in the function of *SMC2* or *SMC4* have been reported to cause mis-segregation of mitotic and meiotic chromosomes in *A. thaliana*. In particular, double *SMC2* mutants showed impaired male and female gametogenesis, embryo lethality and developmental defects [77]. *VIT_12s0028g00110* (with a G > A SNP chr12:766,875) encode a protein that is annotated as a cyclin-dependent kinase (*CDK*), *CYCL1-1/RCY1/MOS12* homolog, a cognate cyclin for *CDKG1* required for synapsis and male meiosis [78]. *CDK*—cyclin complexes also regulate progression through the meiotic

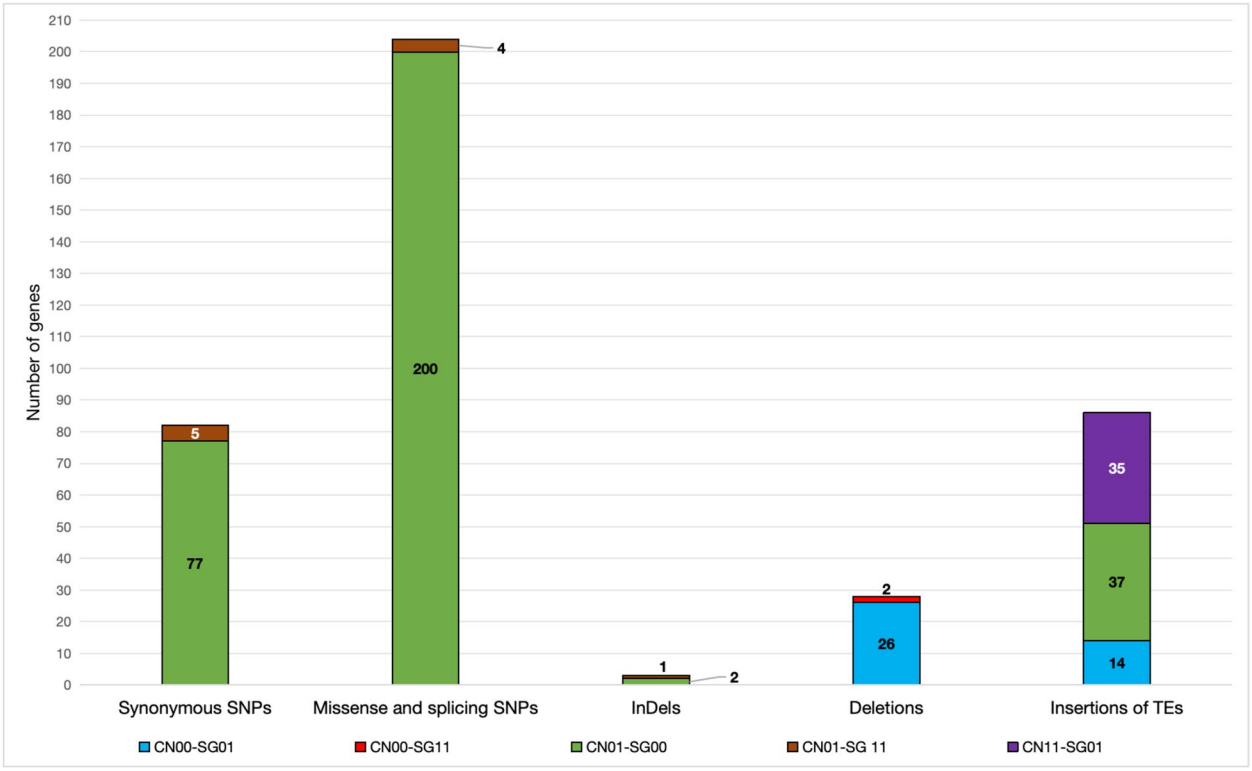

Fig. 7 Distribution of the 403 overall genes overlapping genomic regions for which putative single nucleotide polymorphisms (SNPs), small insertion/deletions (InDels) or structural variations (SV) — deletions, and transposable elements (TEs) insertions - were found between Corinto Nero and Sangiovese seeded clones

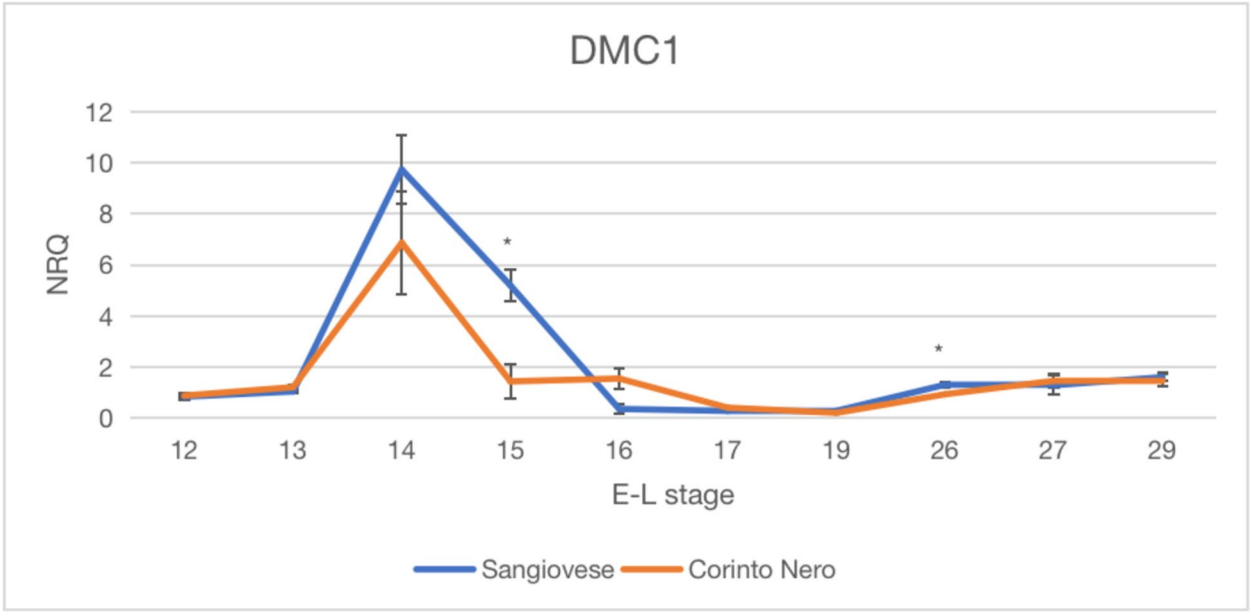

Fig. 8 Expression of the *VIT_05s0020g04170* gene (*DMC1* homolog) in the seedless mutant Corinto Nero (CN) in comparison with the seeded Sangiovese R24 clone (R24) at ten phenological stages. The asterisk (*) indicates the phenological stages for which statistically significant differences in the expression level were detected between R24 and CN according to the T-test ($p < 0.05$)

cell division at key checkpoints [54, 79]. For instance, CDK1 is involved in activation of the Anaphase Promoting Complex/Cyclosome (APC/C) [80], which controls cell cycle transitions [81]. Inhibition of APC-C by the Spindle Assembly Checkpoint (SAC) is enforced until all of the sister chromatids are attached to the mitotic spindle, and then lifted. This way, SAC ensures the correct attachment of microtubules to kinetochores in the metaphase to anaphase transition, thus ensuring faithful chromosome segregation [54, 79, 82]. The G > A SNP chr5:2,962,594 is in the gene *VIT_05s0020g01200*, which encodes a kinesin family member 2/24. Kinesins are cytoskeletal motor proteins that are involved in chromosome segregation during mitosis and meiosis. The Arabidopsis Kinesin-13A (AtKIN13) is specifically associated with Golgi vesicles. Strong reductions in the activity of AtKIN13 proteins cause gametophytic defects and embryo lethality [83, 84]. *VIT_07s0205g00140*, which harbors a homozygous TE insertion in CN, is also annotated as a kinesin-like protein and its Arabidopsis orthologue (*KIN8B*) is required for spindle assembly [85]. The A > T SNP chr12:16,763,035 involves the *VIT_12s0034g00950* gene that also encodes for a kinetochore protein. The product of its *A. thaliana* ortholog gene encodes a unit of the NDC80 complex. This protein complex has roles not only in assembling the structure of the kinetochore, but also in chromosomes congression and spindle checkpoint signaling [86, 87]. Checkpoints are regulatory mechanisms that arrest or delay meiotic cell cycle progression when key cellular processes are defective or chromosomes are damaged, thus preventing the formation of imbalanced gametes. However, the meiotic cell cycle control appears to be set less tightly in plants compared to yeast and animals [88].

Other factors, such as environmental stresses, might also influence chromosome segregation in plant meiosis [54], as well as cell cycle control and gametophyte development. Consistently, we found putative mutations in candidate genes belong to the "response to stress" and "response to stimulus" categories (Fig. 6, Supplementary Material 20). The C > A SNP chr3:4,108,589 affects *VIT_03s0063g00600*, which is related to autophagy and senescence. Autophagy is required for efficient meiosis progression and correct chromosome segregation in fission yeast [89]. Two SNPs, one A > T substitution at chr6:6,524,413 and one C > G substitution at chr8:14,520,767, are located in the *VIT_06s0004g05770* and *VIT_08s0007g00130* genes, respectively, that are related to heat stress. The former encodes a heat shock protein 17.6 kDa class I (Hsp17.6I) involved in pollen germination and tube growth [90]; while the latter encodes a heat shock protein 70 (Hsp70). Hsp70 acts in chaperone cofactor-dependent protein refolding processes and, together with Hsp110, is required to ensure correct spindle assembly and nuclear division. The modulation of spindle length by molecular chaperones might be a mechanism by which cell division can be controlled under proteostatic stress [91]. In addition, a C > T SNP chr18_random:4,858,038 affects the gene *VIT_18s0001g06480*, an aquaporin *PIP1-3* homolog related to water stress. Aquaporins play a role in anther dehydration, pollen development, hydration and germination, and pollen tube elongation [92]. An Arabidopsis *PIP1;5* quintuple mutant is disturbed in the normal dehydration and maturation process of pollen grains and exhibits an abnormal pollen exine shape, as well as reduced vitality and germination rates [93]. On the other hand, the *VIT_14s0006g01850* gene carrying a A > G SNP chr14:18,458,177, encodes an Exportin 1 protein (*XPO1*), which functions as a receptor for nuclear export. The product of the ortholog *AtXPO1A* gene is sensitive to heat and oxidative stress, and binds to a variety of proteins having leucine rich export signals. Along with *XPO1B*, it is involved in the development of male and female gametophytes [94]. An *A. thaliana* ortholog of the *VIT_08s0007g03610* gene (with a A > G SNP chr8:17,562,688) encodes a peroxisomal monodehydroascorbate reductase (*AtMDAR1*) involved in the ascorbate–glutathione cycle, which removes toxic H_2O_2. Besides the implication of ascorbate and glutathione in the defense against oxidative stress, these two compounds are also involved in plant growth and cell cycle control. Ascorbate metabolism is closely linked to the development of embryos and seedlings. Furthermore, ascorbate stimulates cell cycle activity in competent cells, while the oxidized form blocks normal cell cycle progression [95].

Epigenetic regulatory pathways, in particular those involved in DNA methylation and small RNA-based gene regulation, are important for germline specification and the control of sexual reproduction versus apomixis [96]. *VIT_19s0014g01500* is affected by a G > A SNP chr19:1,606,950 and is putatively involved, besides histone acetylation, in DNA methylation and gene silencing by RNA-directed DNA methylation processes. Its *A. thaliana* ortholog, the *Increased DNA methylation 1* gene (*AtIDM1*, a histone H3 acetyltransferase) negatively regulates DNA demethylation, preventing DNA hypermethylation of highly homologous multicopy genes and other repetitive sequences. Interestingly, methylation of this gene has been linked to differences in reproductive modes in the comparison between apomictic and sexual genotypes of the diplosporous grass *Eragrostis curvula* species [97]. *VIT_15s0024g00700* (with an InDel in chr5:1,168,070 causing a frameshift mutation) codes for a Lysine-tRNA ligase. In Arabidopsis lysine-tRNA ligases are related to gametogenesis and embryo development [98] and its homolog in the *Limonium* genus was

differentially expressed in ovules between apomictic and sexual plants [99].

Other candidate genes for having a role in apomixis are *VIT_02s0033g00080* and *VIT_02s0033g00120* (harbored in a MSV region, Supplementary Material 27), which have similarity with the *APOSTART* gene. Based on *APOSTART1* and *APOSTART6* differential expression between *Poa pratensis* apomictic and sexual genotypes, this gene was proposed to have a role in microspores, in the programmed cell death of non-functional megaspores and in nucellar cell degeneration events that permit embryo sac enlargement [100, 101]. A crucial role of *APOSTART* in the formation of seeds by apomixis was strengthened by its expression profile in other apomictic species [102]. The Arabidopsis *APOSTART1* ortholog was found to be expressed in mature female embryo sacs and developing embryos, and the phenotype of *APOSTART1/APOSTART2* double mutants suggested for this gene a role in embryo and seed development [103].

Other candidate genes are involved in different ways in the next steps of gametophyte development. *VIT_05s0020g01550* (with a G>A SNP chr5:3,230,483), encodes an isoleucyl-tRNA synthetase with a role in translation. Its *A. thaliana* ortholog, *Ovule abortion 2* gene (*AtOVA2*), may suggest a role in gametogenesis and female gametophyte development [98]. *VIT_18s0001g02090* (with a homozygous TE insertion in CN) corresponds to *REPLICATIPON FACTOR C4* (*EMBRYO DEFECTIVE 1968*), which is indispensable for DNA replication and functions in both endosperm and embryo development [104]. On the other side, *VIT_02s0154g00090* (with a C>T SNP chr2:4,882,706) and *VIT_12s0178g00190* (with a A>G SNP chr12:8,663,241) are putatively involved in pollen development [105, 106]. In the latter gene, a heterozygous InDel was also identified in the parthenocarpic mutant of ARI 516 [30].

Finally, a few candidates were identified owing to their role in response to hormones. *VIT_16s0013g00950* (affected by a G>A SNP chr16:6,676,634) encodes an ethylene-responsive transcription factor *ERF105* (*VvERF080*). The higher expression observed in CN than in SG at stage E-L26 (Fig. 8) [29] is fully consistent with the higher expression levels found for this gene in seedless cultivars compared to seeded ones during ovule development after anthesis. This supports a possible role in ovule abortion related to seedlessness [107]. *VIT_01s0244g00150* (with a C>T SNP chr1:21,724,007) is annotated as the auxin response factor *VvARF1* [108]. Auxin is a key regulator of floral meristem and floral organ identity genes [109] and controls the patterning of the female gametophyte [110]. Along with gibberellins and cytokinins, auxins are also required for fruit set in grapevine, and consequently parthenocarpic fruit development may be triggered by a disruption in the balance of these hormones in ovary tissues [111, 112]. Interestingly, gene expression data in apomictic genotypes compared to genotypes that necessarily require fertilization to produce seeds have also been suggested that hormone signalling plays a role in the control of apomixis by interacting with chromatin regulation and Reacting Oxygen Species effectors [113].

Bicarpellate and tricarpellate flowers in seeded Sangiovese

A bicarpelar and syncarpous ovary is commonplace in the *Vitis* genus [22]. Tricarpellate or multicarpellate ovaries and/or the presence of more than four seeds per berry has been previously observed in other *V. vinifera* cultivars [21, 114–116] and in *Vitis labrusca* [117]. Houel et al. [114] reported that 29% of 180 V. *vinifera* cultivars analyzed formed tricarpellate flowers, with variation in the proportion of bicarpellate and tricarpellate ovaries among- and within-cultivars. The presence of tricarpellate ovaries in 20% of the flowers in R24, which therefore contained six ovules instead of four, agrees with what previously observed [28]. In terms of reproductive capacity, cultivars containing only this type of flowers would have theoretically a 1.5-fold higher fecundity and, hence, potentially deliver higher yield [118]. This feature might, at least in part, explain the higher fruit set rate and less coulure that is observed in SG with respect to other varieties [119]. Interestingly, tricarpellate ovaries were not observed in any of the flowers from CN, which could indicate that it probably does not exhibit this characteristic, although examination of a larger sample would be necessary to exclude a sample size bias.

The carpel is the last flower whorl to develop and C-class genes of the ABCDE model, such *VvAGAMOUS 1 and 2* (*VvAG1, VIT_12s0142g00360*, and VvAG2, *VIT_10s0003g02070*) determine carpel identity and promote carpel development [120], in concert with downstream targets like *VvCRABS CLAW* (*VvCRC*, *VIT_01s0011g00140*) [116]. The heterologous overexpression of *VvAG2* in tomato increased the number of carpels and ovules in the genetically modified plants and, interestingly, all those transgenic lines do not produce seeds [121]. In grapevine, the *VvSUPERMAN*-like gene (*VvSUP*-like, *VIT_05s0049g00070*) is differentially expressed between two- and three-carpel florets in the Xiangfei cultivar and negatively regulates the number of carpels by inhibiting the feedback signaling between *VvAG1* and *VvWUS* (*VvWUSCHEL*, *VIT_04s0023g03300*) expression [122], while *VvWUS* increases carpel number by upregulating *VvAG2* expression [123]. In a previous study [29], we noted a significantly higher expression of *VvAG1* and *VvAG2* in R24 compared to CN at stage E-L15. Further investigation is necessary to elucidate the genetic regulation of this

phenomenon in SG and to assess whether the absence of tricarpellate flowers and the expression of parthenocarpy in CN could be somehow related.

Conclusions

We have observed that ovules in CN do not contain a mature embryo sac at anthesis due to an impaired progression of meiosis, which adds to the already known male sterility [27]. We hypothesize that sterility is the result of a more severe syndrome of a disorder that was already manifest in SG. One or more somatic mutations could have worsened this condition, causing a shift from facultative parthenocarpy present in SG to obligate parthenocarpy in CN, similarly to what happens in other species [124, 125]. The genes underlying seed development, in which we have identified putative mutations, could be targeted for genome editing to functionally validate their association with the CN phenotype or to generate seedless versions of existing seeded varieties, as reported in other species [126, 127]. The application of third-generation sequencing technologies, which in recent years empowered the exploration of previously inaccessible portions of the genomes and the detection of chromosomal rearrangements and large events of presence/absence variation, could reveal other factors potentially responsible for parthenocarpy in CN.

Supplementary Information

The online version contains supplementary material available at https://doi.org/10.1186/s12870-025-07498-3.

Supplementary Material 1. Phenological stages sampled for histological and quantitative RT-PCR expression analyses.

Supplementary Material 2. Quantitative RT-PCR expression analysis of *DMC1* gene and primers' sequences used.

Supplementary Material 3. Summary table of the histological analysis.

Supplementary Material 4. Longitudinal sections of ovules of Sangiovese seedless mutant, Corinto Nero, at stage E-L15.

Supplementary Material 5. Longitudinal sections of different ovules (A, B, C and D) of Sangiovese R24 seeded clone at stage E-L15+2.

Supplementary Material 6. Longitudinal sections of different ovules of Corinto Nero at stage E-L15+2.

Supplementary Material 7. Transversal sections of Corinto Nero at stage E-L15+4.

Supplementary Material 8. Longitudinal sections of flowers of Corinto Nero.

Supplementary Material 9. Longitudinal sequential sections of an ovule of Sangiovese R24 at stage E-L15+7.

Supplementary Material 10. Longitudinal sections of Corinto Nero at stage E-L15+7.

Supplementary Material 11. Transversal serial sections (from left to right) of one ovule of Sangiovese R24 seeded clone at stage E-L15+12.

Supplementary Material 12. Two longitudinal serial sections (from left to right) of one ovule of Sangiovese R24 seeded clone at stage E-L15+14 showing embryo sac structures.

Supplementary Material 13. Longitudinal serial sections (from left to right, A → F) of one of the six ovules of Sangiovese R24 seeded clone at stage E-L15+14.

Supplementary Material 14. Sequential transversal sections, from left to right, of one ovule of Corinto Nero at stage E-L15+12.

Supplementary Material 15. Sequential transversal sections, from left to right, of another ovule of Corinto Nero at stage E-L15+12.

Supplementary Material 16. Sequential transversal sections, from left to right, of another ovule of Corinto Nero at stage E-L15+12.

Supplementary Material 17. Longitudinal sections of three different ovules of Corinto Nero at stage E-L15+14.

Supplementary Material 18. Transversal (A - C) and longitudinal (D - F) sections of different ovules of Corinto Nero at stage E-L15+16.

Supplementary Material 19. Longitudinal sections of two ovules (A, B) of Corinto Nero at stage E-L15+16.

Supplementary Material 20. Longitudinal sections of three different ovules (A - B, C - D and E) of Corinto Nero at stage E-L15+19.

Supplementary Material 21. List of 4513 putative SNPs isolated by GATK Unified Genotyper v2.0.

Supplementary Material 22. List of gene ontology (GO) terms according to the biological process (BP) aspect present among the genes overlapping the putative splicing and exonic missense, stop-gain and stop-loss SNPs and their distribution among them.

Supplementary Material 23. List of 1038 InDels remaining after filtering out read missalignments.

Supplementary Material 24. List of 92 deletions detected.

Supplementary Material 25. List of the 433 TE insertions detected between the ten Sangiovese seeded clones and Corinto Nero.

Supplementary Material 26. List of gene ontology (GO) terms regarding biological processes (BP) present among the 37 genes overlapping the putative TE insertions detected with an assigned genotype of 0/0 and 0/1 for Sangiovese seeded clones (SG) and Corinto Nero (CN), respectively.

Supplementary Material 27. List of gene ontology (GO) terms regarding biological processes (BP) present among the 35 genes overlapping the putative TE insertions detected with an assigned genotype of 0/1 and 1/1 for Sangiovese seeded clones (SG) and Corinto Nero (CN), respectively.

Supplementary Material 28. List of MSV regions detected in each of the Sangiovese seeded clones when compared against Corinto Nero.

Supplementary Material 29. Candidate genes mentioned in the main text that are harbored within the confidence intervals of previoulsy identified QTLs for fertility, seed content and berry size, as reported by Delfino et al. 2019.

Supplementary Material 30. Experimental validation by Sanger sequencing of the non-synonymous SNP chr5:5814092 C>T (in the VIT_05s0020g04170 gene).

Acknowledgements

We want to thank Anna Schneider and Ivana Gribaudo from the CNR-IPSP (National Research Council of Italy-Institute for Sustainable Plant Protection, Torino) for providing the grafts of Sangiovese R24 and Corinto Nero clones. Ph.D. Rosella Tomazzoli, head of the Biotechnology laboratories, and Malgorzata Kos from the University of Trento (Italy) for their technical support on the use of the optical microscope. Ph.D. Y. Wang for the support with the input data elaboration for ShinyCircosv.2. Michela Bernini for her support in the lab.

Authors' contributions

PM-S.: histological analysis, laboratory and data analysis and writing. LC.: SNP validation and expression analysis, data analysis, writing and text revision. SL. and TR.: sample collection and laboratory support. ED.: histological analysis.

MM., GM, GDG: sequencing and bioinformatics analysis of genomic variation and text revision. AN.: histological analysis and text revision. MSG.: supervision, project administration, funding acquisition and text revision. All authors discussed and approved the final manuscript.

Funding
This work was performed with the financial support provided by Fondazione CARITRO (Post-Doc project APIRENIA, int. ref. 2017.0349) and by the Autonomous Province of Trento (Accordo di Programma).

Data availability
The data of this article are available in the main text and in supplementary material. Raw reads are deposited in the NCBI short read archive under the BioProject numbers PRJNA1277789 and PRJNA1277790.

Declarations

Ethics approval and consent to participate
Not applicable.

Consent for publication
Not applicable.

Competing interests
The authors declare no competing interests.

Author details
[1]Center Agriculture Food Environment (C3A), University of Trento, San Michele All'Adige, Trento, Italy
[2]Research and Innovation Centre, Fondazione Edmund Mach, San Michele All'Adige, Trento, Italy
[3]Department of Physics, University of Trento, Povo, Trento, Italy
[4]Technology Transfer Center, Fondazione Edmund Mach, San Michele All'Adige, Trento, Italy
[5]Department of Agricultural, Food, Environmental and Animal Sciences, University of Udine, Udine 33100, Italy
[6]Istituto Di Genomica Applicata, Udine 33100, Italy
[7]Departamento de Viticultura, Instituto de Ciencias de La Vid y del Vino (CSIC, UR, Gobierno de La Rioja), Logroño, Spain
[8]Department of Genetics and Cytology, Yerevan State University, Yerevan, Armenia
[9]Present address: Biological and Environmental Science and Engineering Division, King Abdullah University of Science and Technology (KAUST), Thuwal, Makkah 23955-6900, Kingdom of Saudi Arabia

Received: 19 June 2025 / Accepted: 26 September 2025
Published online: 22 November 2025

References

1. Carbonell-Bejerano P, Royo C, Mauri N, Ibáñez J, Miguel Martínez Zapater J. Somatic variation and cultivar innovation in grapevine. In: Morata A, Loira I, editors. Advances in grape and wine biotechnology. IntechOpen; 2019. https://doi.org/10.5772/intechopen.86443.
2. Ban S, Jung JH. Somatic mutations in fruit trees: causes, detection methods, and molecular mechanisms. Plants. 2023;12:1316.
3. Emanuelli F, Battilana J, Costantini L, Le Cunff L, Boursiquot JM, This P, et al. A candidate gene association study on muscat flavor in grapevine (*Vitis vinifera* L.). BMC Plant Biol. 2010;10:241.
4. Pelsy F, Dumas V, Bévilacqua L, Hocquigny S, Merdinoglu D. Chromosome replacement and deletion lead to clonal polymorphism of berry color in grapevine. PLoS Genet. 2015;11(4):e1005081. https://doi.org/10.1371/journal.pgen.1005081.
5. Ferreira V, Pinto-Carnide O, Arroyo-García R, Castro I. Berry color variation in grapevine as a source of diversity. Plant Physiol Biochem. 2018;132:696–707.
6. Huang J, Zhang G, Li Y, Lyu M, Zhang H, Zhang N, et al. Integrative genomic and transcriptomic analyses of a bud sport mutant "Jinzao Wuhe" with the phenotype of large berries in grapevines. PeerJ. 2023;11:e14617. https://doi.org/10.7717/peerj.14617.
7. Boss PK, Thomas MR. Association of dwarfism and floral induction with a grape 'green revolution' mutation. Nature. 2002;416:847–50.
8. Carbonell-Bejerano P, Royo C, Torres-Pérez R, Grimplet J, Fernandez L, Franco-Zorrilla JM, et al. Catastrophic unbalanced genome rearrangements cause somatic loss of berry color in grapevine. Plant Physiol. 2017;175:786–801.
9. Tello J, Royo C, Baroja E, García-Escudero E, Martínez-Zapater JM, Carbonell-Bejerano P. Reduced gamete viability associated to somatic genome rearrangements increases fruit set sensitivity to the environment in Tempranillo Blanco grapevine cultivar. Sci Hortic. 2021;290:110497. https://doi.org/10.1016/j.scienta.2021.110497.
10. Kobayashi S, Goto-Yamamoto N, Hirochika H. Retrotransposon-induced mutations in grape skin color. Science. 2004;304:982.
11. Fernandez L, Torregrosa L, Segura V, Bouquet A, Martinez-Zapater JM. Transposon-induced gene activation as a mechanism generating cluster shape somatic variation in grapevine. Plant J. 2010;61:545–57.
12. Fernandez L, Chäib J, Martinez-Zapater JM, Thomas MR, Torregrosa L. Mis-expression of a PISTILLATA-like MADS box gene prevents fruit development in grapevine. Plant J. 2013;73:918–28.
13. Torregrosa L, Fernandez L, Bouqeut A, Boursiquot J-M, Frédérique P, Zapater J. Origins and consequences of somatic variation in grapevine. In: Genetics, genomics, and breeding of grapes. 2011. pp. 68–92.
14. Carrier G, Le Cunff L, Dereeper A, Legrand D, Sabot F, Bouchez O, et al. Transposable elements are a major cause of somatic polymorphism in *Vitis vinifera* L. PLoS ONE. 2012;7(3):e32973. https://doi.org/10.1371/journal.pone.0032973.
15. Urra C, Sanhueza D, Pavez C, Tapia P, Núñez-Lillo G, Minio A, et al. Identification of grapevine clones via high-throughput amplicon sequencing: a proof-of-concept study. G3. 2023;13(9):jkad145.
16. Ledbetter CA, Ramming DW. Seedlessness in Grapes. In: Horticultural Reviews. John Wiley & Sons, Ltd; 1989. p. 159–84.
17. Royo C, Torres-Pérez R, Mauri N, Diestro N, Cabezas JA, Marchal C, et al. The major origin of seedless grapes is associated with a missense mutation in the MADS-Box gene *VviAGL11*. Plant Physiol. 2018;177:1234–53.
18. Amato A, Cardone MF, Ocarez N, Alagna F, Ruperti B, Fattorini C, et al. *VviAGL11* self-regulates and targets hormone- and secondary metabolism-related genes during seed development. Hortic Res. 2022;9:uhac133. https://doi.org/10.1093/hr/uhac133.
19. Kim MS, Hur YY, Kim JH, Jeong SC. Genome resequencing, improvement of variant calling, and population genomic analyses provide insights into the seedlessness in the genus *Vitis*. G3 Genes|Genomes|Genetics. 2020;10:3365–77.
20. Wang X, Liu Z, Zhang F, Xiao H, Cao S, Xue H, et al. Integrative genomics reveals the polygenic basis of seedlessness in grapevine. Curr Biol. 2024;34:3763–77.
21. Stout AB. Seedlessness in grapes. N Y State Agric Exp Stn Tech Bull. 1936;238:68.
22. Pratt C. Reproductive anatomy in cultivated grapes: a review. Am J Enol Vitic. 1971;22:92–109.
23. Royo C, Carbonell-Bejerano P, Torres-Pérez R, Nebish A, Martínez Ó, Rey M, et al. Developmental, transcriptome, and genetic alterations associated with parthenocarpy in the grapevine seedless somatic variant Corinto bianco. J Exp Bot. 2016;67:259–73.
24. Vouillamoz JF, Monaco A, Constantini L, Stefanini M, Scienza A, Grando MS. The parentage of "Sangiovese", the most important Italian wine grape. VITIS - J Grapevine Res. 2007;46:19–22.
25. Schneider A, Raimondi S, Moreira FM, De Santis D, Zappia R, Torello Marinoni D, et al. Contributo all'identificazione dei principali vitigni calabresi. Frutticoltura. 2009;71:46–55.
26. Gristina A, De Michele R, Garfì G, La Mantia T, Fontana I, Spinelli P, et al. Urgent need for preservation of grapevine (*Vitis vinifera* L. subsp. *vinifera*) germplasm from small circum-Sicilian islands as revealed by SSR markers and traditional use investigations. Genet Resour Crop Evol. 2017;64:1395–415.
27. Costantini L, Moreno-Sanz P, Nwafor CC, Lorenzi S, Marrano A, Cristofolini F, et al. Somatic variants for seed and fruit set in grapevine. BMC Plant Biol. 2021;21:1–33.
28. Moreno-Sanz P, D' Amato E, Nebish A, Costantini L, Grando MS. An optimized histological proceeding to study the female gametophyte development in grapevine. Plant Methods. 2020;16:61.
29. Nwafor CC, Gribaudo I, Schneider A, Wehrens R, Grando SM, Costantini L. Transcriptome analysis during berry development provides insights into co-regulated and altered gene expression between a seeded wine grape variety and its seedless somatic variant. BMC Genomics. 2014;15:1030.

30. Chavan S, Phalake S, Tetali S, Barvkar VT, Patil R. Comparative gametogenesis and genomic signatures associated with pollen sterility in the seedless mutant of grapevine. BMC Plant Biol. 2025;25:138.
31. Coombe BG. Growth stages of the grapevine: adoption of a system for identifying grapevine growth stages. Aust J Grape Wine Res. 1995;1:104–10.
32. Schindelin J, Arganda-Carreras I, Frise E, Kaynig V, Longair M, Pietzsch T, et al. Fiji: an open-source platform for biological-image analysis. Nat Methods. 2012;9:676–82.
33. Doyle JJ, Doyle JL. A rapid DNA isolation procedure for small quantities of fresh leaf tissue. Phytochem Bull. 1987;19:11–5.
34. Magris G, Jurman I, Fornasiero A, Paparelli E, Schwope R, Marroni F, et al. The genomes of 204 *Vitis vinifera* accessions reveal the origin of European wine grapes. Nat Commun. 2021;12:7240.
35. Van der Auwera GA, O'Connor BD. Genomics in the cloud: using Docker, GATK, and WDL in Terra. 1st ed. Sebastopol: O'Reilly Media; 2020. Print.
36. Vitulo N, Forcato C, Carpinelli EC, Telatin A, Campagna D, D'Angelo M, et al. A deep survey of alternative splicing in grape reveals changes in the splicing machinery related to tissue, stress condition and genotype. BMC Plant Biol. 2014;14:99.
37. Rausch T, Zichner T, Schlattl A, Stütz AM, Benes V, Korbel JO. DELLY: structural variant discovery by integrated paired-end and split-read analysis. Bioinformatics. 2012;28:333–9.
38. Pinosio S, Giacomello S, Faivre-Rampant P, Taylor G, Jorge V, Le Paslier MC, et al. Characterization of the poplar pan-genome by genome-wide identification of structural variation. Mol Biol Evol. 2016;33:2706–19.
39. Marroni F, Scaglione D, Pinosio S, Policriti A, Miculan M, Di Gaspero G, et al. Reduction of heterozygosity (ROH) as a method to detect mosaic structural variation. Plant Biotechnol J. 2017;15:791–3.
40. Scalabrin S, Magris G, Liva M, Vitulo N, Vidotto M, Scaglione D, et al. A chromosome-scale assembly reveals chromosomal aberrations and exchanges generating genetic diversity in *Coffea arabica* germplasm. Nat Commun. 2024;15:463.
41. Wang Y, Jia L, Tian G, Dong Y, Zhang X, Zhou Z, et al. ShinyCircos-V2.0: leveraging the creation of circos plot with enhanced usability and advanced features. iMeta. 2023;2:e109.
42. Howe KL, Achuthan P, Allen J, Allen J, Alvarez-Jarreta J, Amode MR, et al. Ensembl 2021. Nucleic Acids Res. 2021;49(D1):D884–91. https://doi.org/10.1093/nar/gkaa942.
43. Ashburner M, Ball CA, Blake JA, Botstein D, Butler H, Cherry JM, et al. Gene ontology: tool for the unification of biology. Nat Genet. 2000;25:25.
44. Consortium TGO, Aleksander SA, Balhoff J, Carbon S, Cherry JM, Drabkin HJ, et al. The gene ontology knowledgebase in 2023. Genetics. 2023;224:iyad031.
45. Consortium TU. Uniprot: the universal protein knowledgebase in 2023. Nucleic Acids Res. 2023;51:523–31.
46. Navarro-Payá D, Santiago A, Orduña L, Zhang C, Amato A, D'Inca E, et al. The grape gene reference catalogue as a standard resource for gene selection and genetic improvement. Front Plant Sci. 2022;12:803977. https://doi.org/10.3389/fpls.2021.803977.
47. Canaguier A, Grimplet J, Di Gaspero G, Scalabrin S, Duchêne E, Choisne N, et al. A new version of the grapevine reference genome assembly (12X.v2) and of its annotation (VCost.v3). Genomics Data. 2017;14:56.
48. Delfino P, Zenoni S, Imanifard Z, Tornielli GB, Bellin D. Selection of candidate genes controlling veraison time in grapevine through integration of meta-QTL and transcriptomic data. BMC Genomics. 2019;20:1–19.
49. Doutriaux MP, Couteau F, Bergounioux C, White C. Isolation and characterisation of the *RAD51* and *DMC1* homologs from *Arabidopsis thaliana*. Mol Gen Genet. 1998;257:283–91.
50. Couteau F, Belzile F, Horlow C, Grandjean O, Vezon D, Doutriaux MP. Random chromosome segregation without meiotic arrest in both male and female meiocytes of a *dmc1* mutant of Arabidopsis. Plant Cell. 1999;11:1623–34.
51. Untergasser A, Cutcutache I, Koressaar T, Ye J, Faircloth BC, Remm M, et al. Primer3–new capabilities and interfaces. Nucleic Acids Res. 2012;40(15):e115. https://doi.org/10.1093/nar/gks596.
52. Tamura K, Stecher G, Peterson D, Filipski A, Kumar S. MEGA6: molecular evolutionary genetics analysis version 6.0. Mol Biol Evol. 2013;30:2725–9.
53. Hall TA. BIOEDIT: a user-friendly biological sequence alignment editor and analysis program for Windows 95/98/ NT. Nucleic Acids Symp Ser. 1999;41:95–8.
54. Zamariola L, Tiang CL, De Storme N, Pawlowski W, Geelen D. Chromosome segregation in plant meiosis. Front Plant Sci. 2014;5:279.
55. Neale MJ, Keeney S. Clarifying the mechanics of DNA strand exchange in meiotic recombination. Nature. 2006;442:153–8.
56. Wang H, Hu Q, Tang D, Liu X, Du G, Shen Y, et al. *OsDMC1* is not required for homologous pairing in rice meiosis. Plant Physiol. 2016;171:230.
57. Colas I, Barakate A, MacAulay M, Schreiber M, Stephens J, Vivera S, et al. Desynaptic5 carries a spontaneous semi-dominant mutation affecting disrupted meiotic cDNA 1 in barley. J Exp Bot. 2019;70:2683–98.
58. Szurman-Zubrzycka M, Baran B, Stolarek-Januszkiewicz M, Kwaśniewska J, Szarejko I, Gruszka D. The Dmc1 mutant allows an insight into the DNA double-strand break repair during meiosis in barley (*Hordeum vulgare* L.). Front Plant Sci. 2019;10:761.
59. Shinoyama H, Ichikawa H, Nishizawa-Yokoi A, Skaptsov M, Toki S. Simultaneous TALEN-mediated knockout of chrysanthemum DMC1 genes confers male and female sterility. Sci Rep 2020 101. 2020;10:16165.
60. Fei X, Shi J, Liu Y, Niu J, Wei A. The steps from sexual reproduction to apomixis. Planta. 2019;249:1715–30.
61. Kobayashi T, Hotta Y, Tabata S. Isolation and characterization of a yeast gene that is homologous with a meiosis-specific cDNA from a plant. Mol Gen Genet. 1993;237:225–32.
62. Klimyuk VI, Jones JDG. AtDMC1, the Arabidopsis homologue of the yeast DMC1 gene: characterization, transposon-induced allelic variation and meiosis-associated expression. Plant J. 1997;11:1–14.
63. Sakane I, Kamataki C, Takizawa Y, Nakashima M, Toki S, Ichikawa H, et al. Filament formation and robust strand exchange activities of the rice DMC1A and DMC1B proteins. Nucleic Acids Res. 2008;36:4266–76.
64. Devisetty UK, Mayes K, Mayes S. The *RAD51* and *DMC1* homoeologous genes of bread wheat: cloning, molecular characterization and expression analysis. BMC Res Notes. 2010;3:245.
65. Etedali F, Baghban Kohnehrouz B, Valizadeh M, Gholizadeh A, Malboobi MA. Genome wide cloning of maize meiotic recombinase Dmc1 and its functional structure through molecular phylogeny. Genet Mol Res. 2011;10:1636–49.
66. Terasawa M, Shinohara A, Hotta Y, Ogawa H, Ogawa T. Localization of RecA-like recombination proteins on chromosomes of the lily at various meiotic stages. Genes Dev. 1995;9:925–34.
67. Kathiresan A, Khush GS, Bennett J. Two rice DMC1 genes are differentially expressed during meiosis and during haploid and diploid mitosis. Sex Plant Reprod. 2002;14:257–67.
68. Okada T, Catanach AS, Johnson SD, Bicknell RA, Koltunow AM. An *Hieracium* mutant, loss of apomeiosis 1 (loa1) is defective in the initiation of apomixis. Sex Plant Reprod. 2007;20:199–211.
69. Mayama T, Ohtsubo E, Tsuchimoto S. Isolation and expression analysis of Petunia CURLY LEAF-like genes. Plant Cell Physiol. 2003;44:811–9.
70. Pradillo M, Knoll A, Oliver C, Varas J, Corredor E, Puchta H, et al. Involvement of the cohesin cofactor PDS5 (SPO76) during meiosis and DNA repair in *Arabidopsis thaliana*. Front Plant Sci. 2015;6:1034.
71. Abdelgawwad MR, Marić A, Al-Ghamdi AA, Hatamleh AA. Interactome analysis and docking sites of MutS homologs reveal new physiological roles in *Arabidopsis thaliana*. Molecules. 2019;24:2493.
72. Lloyd AH, Milligan AS, Langridge P, Able JA. TaMSH7: a cereal mismatch repair gene that affects fertility in transgenic barley (*Hordeum vulgare* L.). BMC Plant Biol. 2007;7:67.
73. Higgins JD, Vignard J, Mercier R, Pugh AG, Franklin FCH, Jones GH. *AtMSH5* partners *AtMSH4* in the class I meiotic crossover pathway in *Arabidopsis thaliana*, but is not required for synapsis. Plant J. 2008;55:28–39.
74. Rosa M, Von Harder M, Aiese Cigliano R, Schlogelhofer P, Mittelsten Scheid O. The Arabidopsis SWR1 chromatin-remodeling complex is important for DNA repair, somatic recombination, and meiosis. Plant Cell. 2013;25(6):1990–2001. https://doi.org/10.1105/tpc.112.104067.
75. Wang J, Gao S, Peng X, Wu K, Yang S. Roles of the INO80 and SWR1 chromatin remodeling complexes in plants. Int J Mol Sci. 2019;20(18):4591. https://doi.org/10.3390/ijms20184591.
76. Zhao L, He J, Cai H, Lin H, Li Y, Liu R, et al. Comparative expression profiling reveals gene functions in female meiosis and gametophyte development in Arabidopsis. Plant J. 2014;80:615–28.
77. Siddiqui NU, Stronghill PE, Dengler RE, Hasenkampf CA, Riggs CD. Mutations in Arabidopsis condensin genes disrupt embryogenesis, meristem organization and segregation of homologous chromosomes during meiosis. Development. 2003;130:3283–95.
78. Zheng T, Nibau C, Phillips DW, Jenkins G, Armstrong SJ, Doonan JH. CDKG1 protein kinase is essential for synapsis and male meiosis at high ambient temperature in *Arabidopsis thaliana*. Proc Natl Acad Sci U S A. 2014;111:2182–7.

79. Subramanian VV, Hochwagen A. The meiotic checkpoint network: step-by-step through meiotic prophase. Cold Spring Harb Perspect Biol. 2014;6(10):a016675. https://doi.org/10.1101/cshperspect.a016675.
80. Fujimitsu K, Grimaldi M, Yamano H. Cyclin-dependent kinase 1-dependent activation of APC/C ubiquitin ligase. Science. 2016;352:1121–4.
81. Willems A, De Veylder L. The plant anaphase-promoting complex/cyclosome. Annu Rev Cell Dev Biol. 2022;38:25–48.
82. Malmanche N, Maia A, Sunkel CE. The spindle assembly checkpoint: preventing chromosome mis-segregation during mitosis and meiosis. FEBS Lett. 2006;580:2888–95.
83. Mucha E, Hoefle C, Hückelhoven R, Berken A. RIP3 and AtKinesin-13A - a novel interaction linking Rho proteins of plants to microtubules. Eur J Cell Biol. 2010;89:906–16.
84. Fujikura U, Elsaesser L, Breuninger H, Sánchez-Rodríguez C, Ivakov A, Laux T, et al. Atkinesin-13A modulates cell-wall synthesis and cell expansion in *Arabidopsis thaliana* via the THESEUS1 pathway. PLoS Genet. 2014;10(9):e1004627. https://doi.org/10.1371/journal.pgen.1004627.
85. Yamada M, Goshima G. Mitotic spindle assembly in land plants: molecules and mechanisms. Biology. 2017;6:6.
86. Du Y, Dawe RK. Maize NDC80 is a constitutive feature of the central kinetochore. Chromosoma Res. 2007;15:767–75.
87. Tooley J, Stukenberg PT. The ndc80 complex: integrating the kinetochore's many movements. Chromosom Res. 2011;19:377–91.
88. Wijnker E, Schnittger A. Control of the meiotic cell division program in plants. Plant Reprod. 2013;26:143–58.
89. Matsuhara H, Yamamoto A. Autophagy is required for efficient meiosis progression and proper meiotic chromosome segregation in fission yeast. Genes Cells. 2016;21:65–87.
90. Wang Y, Zhang WZ, Song LF, Zou JJ, Su Z, Wu WH. Transcriptome analyses show changes in gene expression to accompany pollen germination and tube growth in Arabidopsis. Plant Physiol. 2008;148:1201–11.
91. Makhnevych T, Houry WA. The control of spindle length by Hsp70 and Hsp110 molecular chaperones. FEBS Lett. 2013;587:1067–72.
92. Wang Y, Zhao Z, Liu F, Sun L, Hao F. Versatile roles of aquaporins in plant growth and development. Int J Mol Sci. 2020;21(24):9485. https://doi.org/10.3390/ijms21249485.
93. Wang X, Wu Y, Liu Z, Liu T, Zheng L, Zhang G. The *pip1s* quintuple mutants demonstrate the essential roles of *pip1s* in the plant growth and development of Arabidopsis. Int J Mol Sci. 2021;22(4):1669. https://doi.org/10.3390/ijms22041669.
94. Blanvillain R, Boavida LC, McCormick S, Ow DW. Exportin1 genes are essential for development and function of the gametophytes in *Arabidopsis thaliana*. Genetics. 2008;180:1493–500.
95. Potters G, Horemans N, Bellone S, Caubergs RJ, Trost P, Guisez Y, et al. Dehydroascorbate influences the plant cell cycle through a glutathione-independent reduction mechanism. Plant Physiol. 2004;134:1479–87.
96. Schmidt A, Schmid MW, Grossniklaus U. Plant germline formation: common concepts and developmental flexibility in sexual and asexual reproduction. Development. 2015;142:229–41.
97. Carballo J, Zappacosta D, Marconi G, Gallardo J, Di Marsico M, Gallo CA, et al. Differential methylation patterns in apomictic vs. sexual genotypes of the diplosporous grass *Eragrostis curvula*. Plants. 2021;10:946.
98. Berg M, Rogers R, Muralla R, Meinke D. Requirement of aminoacyl-tRNA synthetases for gametogenesis and embryo development in Arabidopsis. Plant J. 2005;44:866–78.
99. Caperta AD, Fernandes I, Conceição SIR, Marques I, Róis AS, Paulo OS. Ovule transcriptome analysis discloses deregulation of genes and pathways in sexual and apomictic *Limonium* species (Plumbaginaceae). Genes. 2023;14:901.
100. Albertini E, Marconi G, Reale L, Barcaccia G, Porceddu A, Ferranti F, et al. SERK and APOSTART. Candidate genes for apomixis in *Poa pratensis*. Plant Physiol. 2005;138:2185–99.
101. Marconi G, Aiello D, Kindiger B, Storchi L, Marrone A, Reale L, et al. The role of APOSTART in switching between sexuality and apomixis in *Poa pratensis*. Genes. 2020;11:941.
102. Marconi G, Sharbel T, Colombo L, Masiero S, Barcaccia G, Galla G, et al. Differential expression in sexual and apomictic genotypes of three model species strengthens a crucial role of APOSTART in the formation of seeds by apomixis. In: International plant and animal genome conference. San Diego, CA, USA; 2013.
103. Barcaccia G, Albertini E. Apomixis in plant reproduction: a novel perspective on an old dilemma. Plant Reprod. 2013;26:159–79.
104. Qian J, Chen Y, Hu Y, Deng Y, Liu Y, Li G, et al. *Arabidopsis* replication factor C4 is critical for DNA replication during the mitotic cell cycle. Plant J. 2018;94:288–303.
105. Koonjul PK, Minhas JS, Nunes C, Sheoran IS, Saini HS. Selective transcriptional down-regulation of anther invertases precedes the failure of pollen development in water-stressed wheat. J Exp Bot. 2005;56:179–90.
106. Scholz P, Pejchar P, Fernkorn M, Škrabálková E, Pleskot R, Blersch K, et al. Diacylglycerol kinase 5 regulates polar tip growth of tobacco pollen tubes. New Phytol. 2022;233:2185–202.
107. Zhu Y, Li Y, Zhang S, Zhang X, Yao J, Luo Q, et al. Genome-wide identification and expression analysis reveal the potential function of ethylene responsive factor gene family in response to *Botrytis cinerea* infection and ovule development in grapes (*Vitis vinifera* L.). Plant Biol. 2019;21:571–84.
108. Wan S, Li W, Zhu Y, Liu Z, Huang W, Zhan J. Genome-wide identification, characterization and expression analysis of the auxin response factor gene family in *Vitis vinifera*. Plant Cell Rep. 2014;33:1365–75.
109. Ellis CM, Nagpal P, Young JC, Hagen G, Guilfoyle TJ, Reed JW. Auxin response factor1 and auxin response factor2 regulate senescence and floral organ abscission in *Arabidopsis thaliana*. Development. 2005;132:4563–74.
110. Pagnussat GC, Alandete-Saez M, Bowman JL, Sundaresan V. Auxin-dependent patterning and gamete specification in the Arabidopsis female gametophyte. Science. 2009;324:1684–9.
111. Lu L, Liang J, Zhu X, Xiao K, Li T, Hu J. Auxin- and cytokinin-induced berries set in grapevine partly rely on enhanced gibberellin biosynthesis. Tree Genet Genomes. 2016;12:41.
112. Sharif R, Su L, Chen X, Qi X. Hormonal interactions underlying parthenocarpic fruit formation in horticultural crops. Hortic Res. 2022;9:uhab024. https://doi.org/10.1093/hr/uhab024.
113. Terzaroli N, Anderson AW, Albertini E. Apomixis: oh, what a tangled web we have! Planta. 2023;257:99.
114. Houel C, Martin-Magniette M-L, Nicolas SD, Lacombe T, Le Cunff L, Franck D, et al. Genetic variability of berry size in the grapevine (Vitis vinifera L.). Aust J Grape Wine Res. 2013;19:208–20.
115. Xing JY, Lu L, Wen TJ, Hu JF. The correlation between VvYABBY5 expression and the ontogeny of tricarpellate fruit in 'Xiangfei' grapevine (Vitis vinifera). J Hortic Sci Biotechnol. 2016;91:308–15.
116. Zhang P, Zhang Y, Zhao Q, Niu T, Wen P, Liang J. *Vvagamous* affect development of four different grape species ovary. Phyton. 2023;92:1125–38.
117. Lewis SE. Seedless fruits Mem Bot Club. 1890;1:141–85.
118. Abiri N, Sinjushin A, Tekdal D, Cetiner S. Evaluation of the possible contribution of various regulatory genes to determination of carpel number as a potential mechanism for optimal agricultural yield. Int J Mol Sci. 2022;23:9723.
119. Ibáñez J, Baroja E, Grimplet J, Ibáñez S. Cultivated grapevine displays a great diversity for reproductive performance variables. Crop Breed Genet Genomics. 2020;2:e200003.
120. Palumbo F, Vannozzi A, Magon G, Lucchin M, Barcaccia G. Genomics of flower identity in grapevine (*Vitis vinifera* L.). Front Plant Sci. 2019;10:316.
121. Wang Y, Liu Z, Wu J, Hong L, Liang J, Ren Y, et al. Mads-box protein complex VvAG2, VvSEP3 and VvAGL11 regulates the formation of ovules in Vitis vinifera l. Cv. 'xiangfei.' Genes. 2021;12:647.
122. Liang J, Guan P, Liu Z, Wang Y, Xing J, Hu J. The VvSUPERMAN-like gene is differentially expressed between bicarpellate and tricarpellate florets of Vitis vinifera L. Cv. "Xiangfei" and its heterologous expression reduces carpel number in tomato. Plant Cell Physiol. 2020;61:1760–74.
123. Wu J, Liu Z, Hu J, Guan P. *VvWUS* increases carpel number by upregulating *VvAG2* expression in grapevine. Plant Cell Rep. 2025;44:136.
124. Mazzucato A, Taddei AR, Soressi GP. The parthenocarpic fruit (pat) mutant of tomato (*Lycopersicon esculentum* Mill.) sets seedless fruits and has aberrant anther and ovule development. Development. 1998;125:107–14.
125. Tiwari A, Vivian-Smith A, Voorrips RE, Habets MEJ, Xue LB, Offringa R, et al. Parthenocarpic potential in *Capsicum annuum* L. is enhanced by carpelloid structures and controlled by a single recessive gene. BMC Plant Biol. 2011;11:143.
126. Moniruzzaman M, Darwish AG, Ismail A, El-kereamy A, Tsolova V, El-Sharkawy I. Seedlessness trait and genome editing—a review. Int J Mol Sci. 2023;24:5660.
127. Chen X, Li Y, Liu M, Ai G, Zhang X, Wang J, et al. A sexually and vegetatively reproducible diploid seedless watermelon inducer via ClHAP2 mutation. Nat Plants. 2024;10:1446–52.

Publisher's Note